UNITED STATES DEPARTMENT OF THE INTERIOR

U.S. GEOLOGICAL SURVEY

Joint-History Summary and Orientation Data for Upper Cretaceous Sandstones, Rawlins and Rock Springs Uplifts, Washakie Basin, Southern Wyoming

by

Marilyn A. Grout[1] and Earl R. Verbeek[1]

Open-File Report 92-388

This report is preliminary and has not been reviewed for conformity with U.S. Geological Survey editorial standards and stratigraphic nomenclature.

[1]Box 25046, MS 913, Denver Federal Center, Denver, CO 80225

1992

CONTENTS

FIGURES

TABLES

JOINT-HISTORY SUMMARY AND ORIENTATION DATA FOR UPPER CRETACEOUS SANDSTONES, RAWLINS AND ROCK SPRINGS UPLIFTS, WASHAKIE BASIN, SOUTHERN WYOMING

By Marilyn A. Grout and Earl R. Verbeek

ABSTRACT

Upper Cretaceous sandstones on the Rawlins and Rock Springs uplifts, along the eastern and western margins, respectively, of the Washakie basin in southern Wyoming, record a complex history of Laramide and post-Laramide fracture events. Seven sets of extension joints are present in these rocks on the Rawlins uplift, whereas six sets have been recognized in the Rock Springs area. The fracture histories of the two uplifts are similar only in part. The oldest set known, a well-formed set of extension joints striking N. 24° E. (median) on the Rawlins uplift, has no known counterpart on the Rock Springs uplift, suggesting that fracture began earlier along the eastern border of the Washakie basin than in areas farther west. Two additional, much younger sets likewise appear unique to one uplift or the other. The remaining ten sets, however--five on each uplift--formed in identical sequence and have comparable orientations in both areas; thus we interpret them in terms of five regional fracture events. Properties of the joints within each set are strongly related to lithology (particularly degree of cementation), layer thickness, and previous fracture history.

INTRODUCTION

This report summarizes results from a reconnaissance study of the fracture network of Upper Cretaceous clastic rocks on the Rawlins and Rock Springs uplifts along the eastern and western margins, respectively, of the Washakie basin in southern Wyoming (fig. 1). The Upper Cretaceous strata of these and nearby areas in Wyoming, Colorado, and Utah are of current interest for their large reserves of natural gas in low-permeability sandstone reservoirs and of methane in coalbeds. Production from both types of reservoir is strongly dependent on fractures, yet little is known about properties of the fracture network in these rocks at the outcrop to reservoir scale. Our work, conducted during the summer of 1988, concentrated on well-exposed sandstone strata of both uplifts; no work was initiated on coal. Documentation of fractures at 42 sites, 21 on each uplift, disclosed a complex fracture history of seven sets of extension joints on the Rawlins uplift and six sets on the Rock Springs uplift. Joint formation began earlier along the eastern margin of the Washakie basin than farther west, as shown by the absence of the earliest set on the Rock Springs uplift. Most of the other joint sets can be correlated from one uplift to the other, suggesting that the sets are of regional extent and that study of their properties in outcrop can provide a guide to predicting and interpreting network properties in correlative reservoir strata at depth.

PRESENT-DAY STRUCTURAL CONFIGURATION

The Washakie basin is one of several structural subbasins of the Greater Green River basin complex that occupies parts of Wyoming, Utah, and Colorado (fig. 1). Upper Cretaceous strata in this region were deposited in a broad structural depression that once stretched north to south across the entire North American Continent (Kauffman, 1985). The subbasins and intervening uplifts present today resulted from structural segmentation of that depression during the Laramide orogeny. Although the term "Laramide" has a controversial history, and both the style and timing of Laramide deformation are much debated in the region, neither of these issues will be explored here; for a summary see Brown (1988).

The Rawlins uplift, a sinuous feature of overall north-to-south trend more than 120 km long, forms the eastern border of the Washakie and Great Divide basins (fig. 1). North of the city of Rawlins, which lies on the west edge of the uplift at the approximate boundary between the two basins, Upper Cretaceous strata dip moderately steeply into the Great Divide basin and overlie a large,

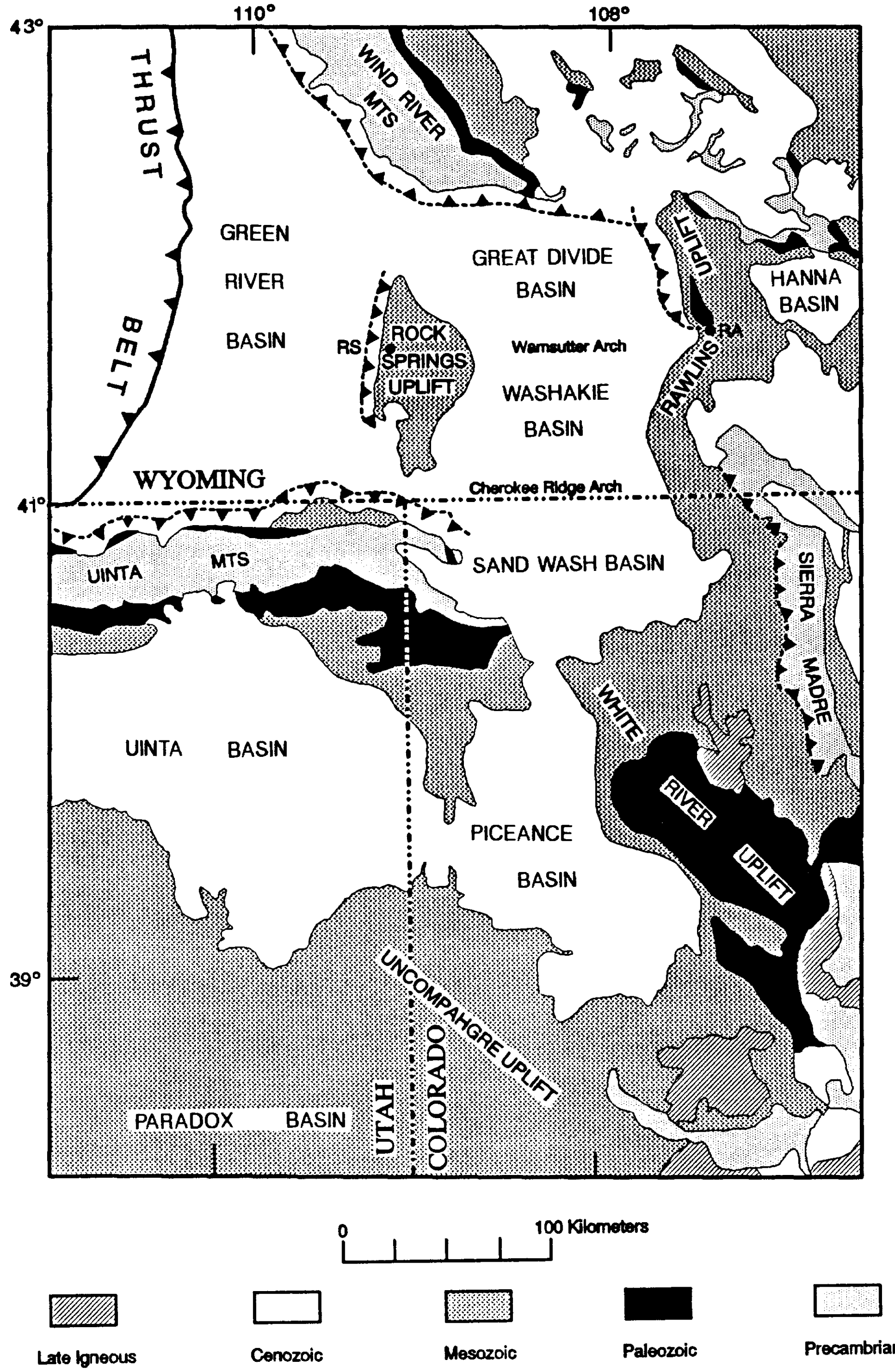

Figure 1. Generalized geologic map of Tertiary basins and uplifts in the central Rocky Mountain foreland, showing location of Rawlins and Rock Springs uplifts relative to Washakie basin in eastern part of Greater Green River basin complex. Inferred traces of major thrust faults (dashed lines, sawteeth on upper plate) are shown only for areas in and near Washakie basin; faults farther south and northeast are omitted. RA, Rawlins; RS, Rock Springs. Modified from Stearns (1978), Love and Christiansen (1985), Bader (1987), Hamilton (1988), and Lickus and Law (1988).

west- to southwest-directed thrust fault at depth (Gries, 1983; Lickus and Law, 1988). South of Rawlins, along the eastern margin of the Washakie basin, the strata dip less steeply, generally 20° or less. Upper Cretaceous strata along this portion of the Rawlins uplift appear relatively little deformed other than by the pervasive network of joints described here and by a few small, high-angle faults of east to northeast trend (Love and Christiansen, 1985).

The Rock Springs uplift, which borders the Washakie and Great Divide basins on the west (fig. 1), brings pre-basin Cretaceous and older strata to the surface over a roughly ovoid area measuring 90 km north to south and 50 km east to west. The uplift is underlain along its western flank by a 64-km long, north-trending, subsurface thrust fault (McDonald, 1975). Joints in Upper Cretaceous strata were measured only along the southeastern flank of the uplift, where the beds dip gently (15° or less) southeastward into the Washakie basin. East-northeast-trending, high-angle normal faults as much as 32 km long are common in this area (Love and Christiansen, 1985; Lickus and Law, 1988).

The other two uplifts bordering the Washakie basin, the Wamsutter arch on the north and the Cherokee Ridge arch on the south (fig. 1), are of lesser amplitude than the Rawlins and Rock Springs uplifts, and no pre-Tertiary rocks crop out along them. Their subsurface configuration is shown on the structure-contour map of Lickus and Law (1988).

STRATIGRAPHY

Upper Cretaceous strata of the Mesaverde Group and overlying Fox Hills Sandstone crop out extensively on both the Rawlins and Rock Springs uplifts. On the Rawlins uplift, these strata extend for 65 km south from Rawlins in a band that varies in width from 3 km to 16 km (fig. 2). From stratigraphically lowest to highest, the Mesaverde Group rocks (table 1) include: (1) the Haystack Mountains Formation, (2) the Allen Ridge Formation, (3) the Pine Ridge Sandstone, and (4) the Almond Formation. These units were combined by Love and Christiansen (1985) and appear as one unit on our base map (fig. 2) and on our tabulated joint data for this area (table 2). Thickness of the Mesaverde Group averages 785 m (Bader, 1987) and of the Fox Hills Sandstone ranges from 46 m to 137 m (Bader, 1987, 1990; Hettinger and Kirschbaum, 1991; Hettinger and others, 1991).

On the Rock Springs uplift, the Upper Cretaceous rocks extend south from the Wamsutter arch for 55 km in a band 8-19 km wide (fig. 3). The Mesaverde Group rocks on the Rock Springs uplift also consist of four formations (table 1); in ascending order, they are: (1) the Blair Formation, (2) the Rock Springs Formation, (3) the Ericson Sandstone, and (4) the Almond Formation. The Blair and the Rock Springs Formations are not present on the Rawlins uplift; the Ericson Sandstone of the Rock Springs area is equivalent to the Haystack Mountains, Allen Ridge, and Pine Ridge Formations farther east. Formations of the Mesaverde Group on the Rock Springs uplift were mapped separately by Love and Christiansen (1985) and are also separated on our tabulated joint data for this area (table 3), but we show only the outcrop belt of the combined Mesaverde Group on the base map of figure 3. Thicknesses for the Mesaverde Group on the Rock Springs uplift range from 1,365 m to 1,705 m and for the Fox Hills Sandstone from 0 m to 75 m (Roehler, 1985).

JOINT STUDY METHODS

Joints in Upper Cretaceous strata of the Rawlins and Rocks Springs uplifts were studied using techniques developed in the Piceance basin farther south (Grout and Verbeek, 1983) and successfully applied to the interpretation of fracture histories there and elsewhere on the Colorado Plateau. The techniques identify each joint set on the basis of its collective characteristics, not just orientation alone, because joint sets of different age commonly have coincident or overlapping orientations in areas of complex fracture history. Moreover, it is rare for any given outcrop to contain all joint sets that developed in a region, and so each locality provides only a partial record of the total deformation history. Accurate interpretation of the evolution of regional fracture systems thus necessitates determination of the sequence in which joint

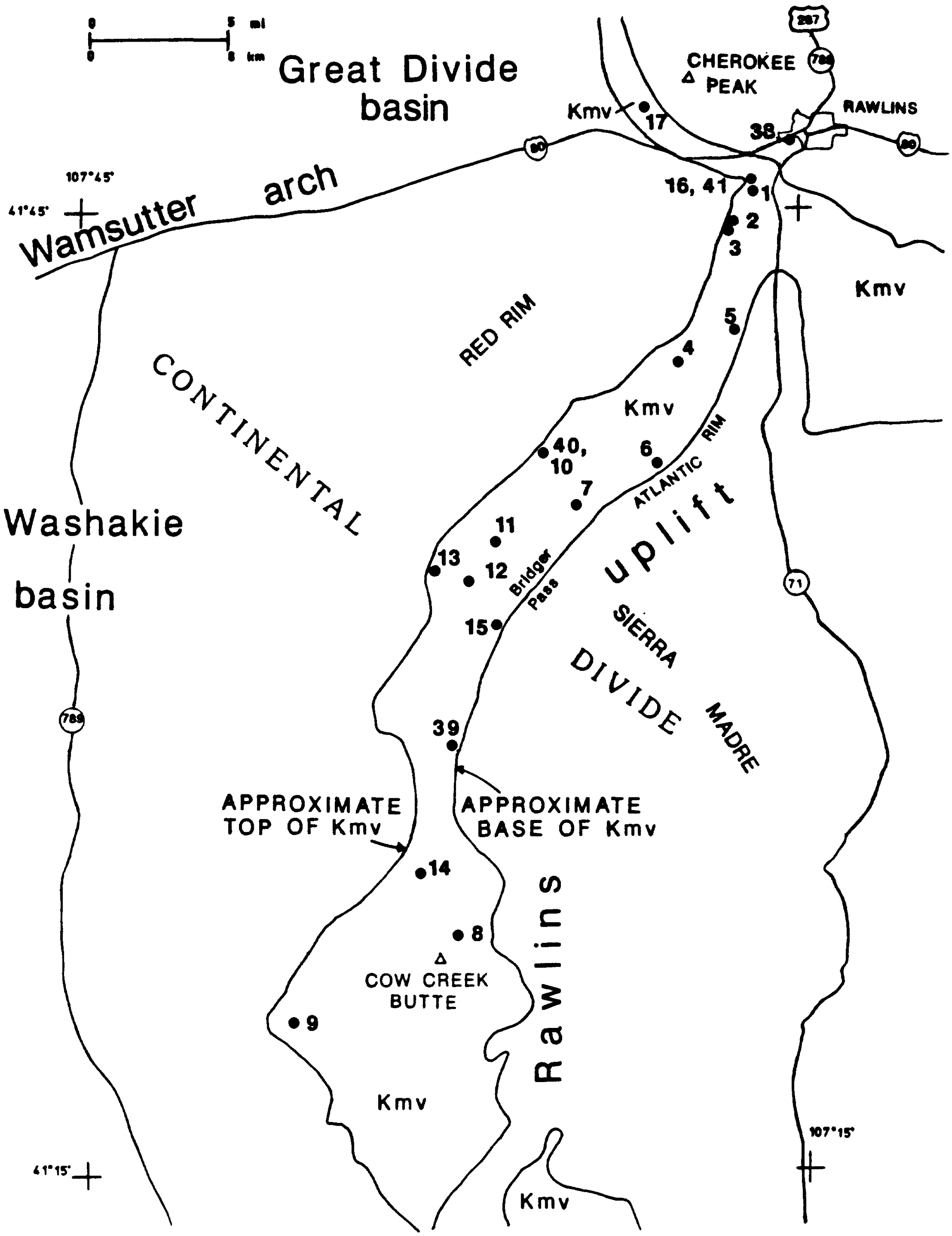

Figure 2. Generalized map of Rawlins uplift along the eastern rim of the Washakie basin, showing outcrop area of the Upper Cretaceous Mesaverde Group (Kmv) and locations of stations (numbered) where joint data were collected.

Table 1. Correlations of Upper Cretaceous strata, listed from stratigraphically highest to lowest, exposed on Rawlins and Rock Springs uplifts along the eastern and western margins, respectively, of the Washakie basin (from Bader and others, 1983; Love and Christiansen, 1985; Lickus and Law, 1988). (X) = formation in which joints were studied.

Rawlins uplift	Rock Springs uplift
Lance Formation	Lance Formation
Fox Hills Sandstone	Fox Hills Sandstone (X)
Lewis Shale	Lewis Shale
Mesaverde Group (X)	Mesaverde Group (X)
Almond Formation (X)	Almond Formation (X)
Pine Ridge Sandstone (X) Allen Ridge Formation (X) Haystack Mountains Formation (X)	Ericson Sandstone (X)
	Rock Springs Formation (X) Blair Formation (X)
Steele Shale	Baxter Shale

Table 2. Station number and set designation for joints in Upper Cretaceous Mesaverde Group rocks on the Rawlins uplift, listed in approximate order from stratigraphically highest to lowest units. (R) = Orientations of joints in tilted beds have been rotated to original bed-horizontal attitudes; (G) = Joint set in Great Divide basin; (C) = Joint set in Cambrian quartzite.

Station no.	Joint-set designation (oldest ——— youngest)						
	F1	F2	F3	F4	F5	F6	F7
1		X	X	X	X		
3 (R)		X			X		
2	X				X		
13	X	X	X		X		
8	X			X	X		
9	X		X		X		
10 (R)					X	X	
40 (R)	X						
4 (R)	X				X		
12 (R)	X		X		X		
14 (R)					X		X
11 (R)	X				X		
17 (R,G)					X	X	
16 (R,G)					X	X	
41 (R,G)					X		X
7 (R)	X						
6 (R)	X		X		X		
5 (R)	X		X				
15 (R)	X		X				
39 (R)	X		X		X		
38 (G,C)	X	(+ 2 older sets)					

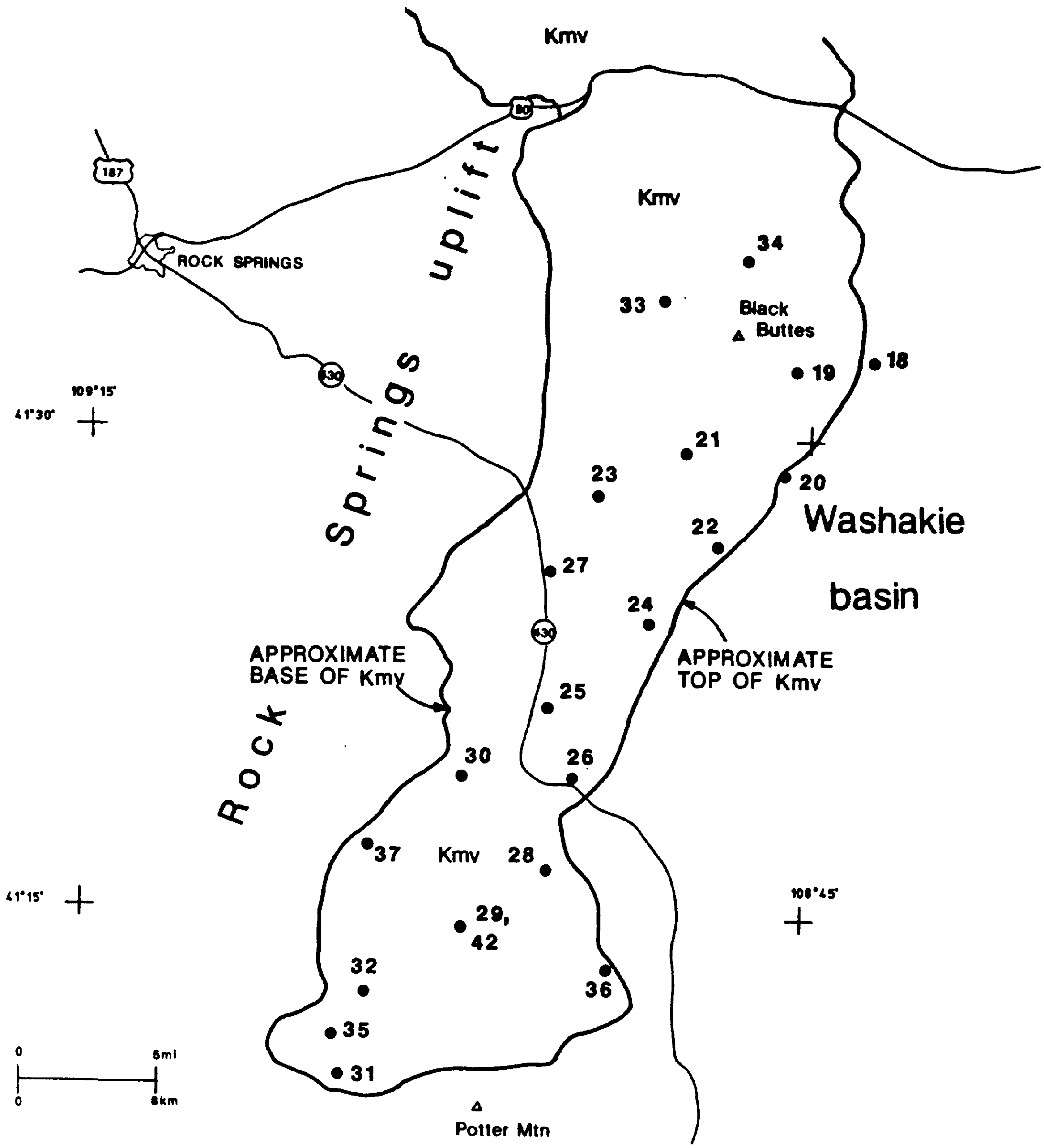

Figure 3. Generalized map of Rock Springs uplift along the western rim of the Washakie basin, showing outcrop area of the Upper Cretaceous Mesaverde Group (Kmv) and locations of stations (numbered) where joint data were collected.

Table 3. Station number, formation name, and set designation for joints in Upper Cretaceous Fox Hills Sandstone and Mesaverde Group strata on the Rock Springs uplift. Formation names are listed from stratigraphically highest to lowest. (R) = orientations of joints of the oldest sets (Fa, Fb, Fd, and Fc) have been rotated to original bed-horizontal orientations. (Note that Fd and Fc sets, though not in alphabetical order, are here listed in probable correct sequence of formation.)

Station no.	Formation name	Joint-set designation					
		oldest ——— youngest					
		Fa	**Fb**	**Fd**	**Fc**	**Fe**	**Ff**
(R) 18	Fox Hills Ss				X		X
(R) 20					X		X
	Mesaverde Group						
28	Almond Fm	X					
(R) 19		X		X			
24		X			X		
26		X		X			
(R) 31			X		X		
36			X		X		
(R) 22						X	
(R) 21	Ericson Ss				X	X	
34				X		X	
35				X			
23	Rock Springs Fm			X		X	
29					X		X
42						X	
(R) 32			X		X		
33				X		X	X
25		X		X			X
27	Blair Fm	X		X	X		
30		X			X		
(R) 37		X			X		

sets developed at each outcrop and accurate correlation of sets from one outcrop to another. Determination of the mode of failure--by extension or shear--is likewise fundamental to interpretation of the mechanical significance of each joint set.

The detailed morphology of fracture surfaces often furnishes the most reliable clue to failure mode. The significance of features such as plumose structure, twist hackle, and arrest lines is treated fully in other papers (Kulander and others, 1979; Pollard and Aydin, 1988) and need not be repeated here, other than to note that all of these features are common on joints of the Rawlins and Rock Springs uplifts and that collectively they are diagnostic of extensile failure of the rock. Slickensided joints are common in a few places as well, but it is important to recognize that these are sheared extension joints and that they did not originate as small faults. The slickenside striations are secondary, a result of thrusting and tilting of beds along the basin margins.

Relative ages of extension-joint sets are determined from the general rule that younger extension joints either terminate against or cut across older ones. Well-developed terminations are common in many places because the tensile stress driving an advancing crack cannot cross the cohesionless boundary represented by an older, open joint. A younger joint can crosscut an older one only where the walls of the pre-existing fracture are bonded together in stress-transmitting contact, generally by minerals precipitated within the intervening open space; however, the mechanical contrast between the wall rock and mineral fill may be sufficient to stop the propagation of the younger joint. Differing proportions of terminating versus crosscutting relations are common among different sets of extension joints in many regions and furnish clues to the mineralization history of an evolving fracture system.

At each study site (joint station), properties measured or described for each joint set include joint orientation, dimensions (length and height), spacing, overall shape, surface features (plumose structure, twist hackle, arrest lines, origin point, slickenside striations), abutting relations with fractures of other sets, mineral filling(s) or coating(s), geometric relation to bedding, and structural relation to dikes and faults. A given set might thus be described as composed of large joints striking N. 10°-25° W., with typical lengths of 3-6 m, heights of 1.5-2 m, spacings of 0.5-1.5 m, well-developed plumose structure and arrest lines, planar surfaces heavily coated with limonite and later calcite, and whose abutting relations with other fractures show them to be the second-oldest of three sets present. The properties and relative ages of the other two sets would be described similarly. In this way a local fracture chronology--a part of the overall, more complex regional chronology--is built for each outcrop. Careful correlation of sets, based on the known sequence of set formation at each locality and consistent with the overall style of each set, then leads to a full interpretation of the evolution of the regional fracture system.

For the purposes of this report, only the orientation of the joints at each outcrop and their relative age on each uplift are listed in the appendix. Orientations of joints in each set are also depicted on Schmidt equal-area plots of poles to joint planes. The joints of all sets originally were nearly vertical, but gentle to moderate basinward tilting of the Cretaceous beds along the basin flanks has rotated the joints of some sets to new attitudes. Actual, present-day orientations of the joints are tabulated in the appendix, but average strikes as shown in the tables are based on original, pre-tilt attitudes for comparison purposes and correlation of sets. Other noteworthy characteristics of the joint sets are summarized in the text. Surficial joints, those that formed during weathering of the rock mass, are not discussed here.

JOINT SETS, RAWLINS UPLIFT

Twenty-one joint stations were established on the Rawlins uplift (fig. 2), twenty in the Upper Cretaceous Mesaverde Group sandstones and one (fig. 2, sta. no. 38) in Cambrian quartzite. Three of the 20 stations in the sandstones (fig. 2, sta. nos. 16, 17, and 41) are located on the southern end of the exposed thrust sheet that borders the southeastern end of the Great Divide basin. In this area, the Upper Cretaceous strata dip between 50° and 60°.

Joints in Upper Cretaceous strata on the Rawlins uplift comprise seven distinct sets, here designated F1 (the oldest) though F7 (the youngest) (table 4). The sets vary widely both in relative abundance and in areal distribution; hence no one outcrop contains joints of all seven sets. Rather, two to four sets are typical of most localities, but the sets are present in sufficiently diverse combinations that an overall fracture chronology can be established and a provisional history interpreted.

F1 set: N. 10°-30° E. Joints of the F1 set are present in more than two-thirds of the outcrops studied (table 2). Several of their properties are a direct consequence of unimpeded joint growth within a rock unit not previously

Table 4. Median strikes and possible correlations between joint sets in the Upper Cretaceous Mesaverde Group on the Rawlins and Rock Springs uplifts. * = Joint set occurring in ≥1/3 of the outcrops studied.

	Rawlins uplift	Rock Springs uplift
oldest	F1 N24E *	- - - -
	F2 N25W	Fa N32W *
	F3 N61W *	Fb N60W
	F4 N79W	- - - -
	F5 N67E *	Fd N66E *
	- - - -	Fc N37E *
	F6 N29W	Fe N29W
youngest	F7 N61W	Ff N71W

fractured: the F1 joints are large and prominent, their surfaces are more nearly planar than those of later joint sets, and they die out laterally as hairline cracks within the body of the rock instead of terminating against other fractures. Limonite in many places forms dark coatings on F1 joint surfaces and impregnates the adjacent wall rock for distances of a few millimeters to several centimeters; liesegang banding parallel to F1 joint walls is common. Replacement pseudomorphs of limonite after tiny euhedral crystals of a mineral no longer present, but probably pyrite, occur on some F1 joints. The filling of some F1 joints with limonite-cemented sand, coarser than the wall rock, is suggestive of an early phase of wall-rock decementation and particle transport (by gravity?) through the fracture set, but we observed such fillings at only one locality (sta. 11, fig. 2). Many of the F1 joints were later filled with calcite and have remained cemented. Few joint-surface structures are preserved on these joints, but hooks of F1 joints into adjacent, nearby members of the same set are common.

F2 set: N. 05°-30° W. Joints of the F2 set are sparsely distributed on the Rawlins uplift and were found at only three outcrops studied (table 2), all relatively high in the Upper Cretaceous section. In general appearance these joints resemble those of the F1 set; they are large, fairly planar, visually prominent fractures. Observed differences include a lack of calcite and only moderate to light limonite staining of F2 joint walls, but F2 joints were observed at so few localities that these properties should not be taken as characteristic. Terminations of F2 joints against members of the F1 set at the single outcrop where both sets were observed together (fig. 2, sta. no. 13) establishes the F2 set as the younger of the two.

F3 set: N. 45°-65° W. Joints of the F3 set are present in 2/5 of the outcrops studied on the Rawlins uplift (table 2). Lateral terminations of F3 joints against F1 joints are common and amply demonstrate the relative age of the two sets, whose joints generally meet at angles of 60° to 90°. Relative ages of the F3 and F2 sets are less certain because of the comparative rarity of the F2 set, but multiple terminations of F3 against F2 joints at the single study site where both sets are prominently developed (fig. 2, sta. no. 1) supports the chronology given here.

The F3 joints at most localities are markedly shorter than joints of the two earlier sets because their lengths were controlled by the spacings between adjacent F1 joints. In some places, however, a few members of the F3 set cut across calcite-cemented F1 joints and have lengths comparable to those of the earlier joints. Relative to joints of the F1 set, the F3 joints generally are noticeably more irregular in shape, more erratically distributed across the outcrop, and show a greater tendency to terminate vertically against contacts between beds of contrasting lithology. Mineral coatings are not preserved on most F3 joints, but some are calcite-filled and moderately limonite-stained where their surfaces are most protected from weathering. Surface features such as plumose structure and arrest lines are more common on F3 joints than on those of earlier sets. Overall, joints of the F3 set are most abundant in the well-cemented, fine-grained sandstones that in many places form caprocks on thicker, and often somewhat coarser grained, sandstone layers.

F4 set: N. 75°-80° W. Joints of the F4 set are sparsely distributed on the Rawlins uplift. They are present in abundance at only two of the outcrops studied (table 2), both high in the Upper Cretaceous section, and at other localities are either absent or too few in number to warrant designation as a set and inclusion in Table 2. Abundant abutting relations clearly establish the young age of the F4 joints relative to the F1 and F2 sets, but their age relative to the F3 set could not be established with certainty. Many F4 joints are short, only 0.2-2 m in length, because they terminate at both ends against pre-existing F1 and F2 joints. Some, however, cut across the older joints and attain lengths of 3-4 m, implying that the earlier joints were mineralized by the time the F4 set formed. Heights vary with bed thickness and generally are 2 m or less, rarely as much as 3 m. Most F4 joints are gently undulatory along strike and have lightly limonite-stained surfaces; mineral fillings were not observed. Arrest lines (the only surface structures found) and common hooks of F4 joints into F2 joints establish the F4 joints as extension fractures.

F5 set: N. 50°-75° E. Joints of the F5 set are present in more than 3/4 of the outcrops studied (table 2) and constitute by far the dominant joints of the Rawlins uplift in terms of numbers and areal extent. Well-formed plumose structure is common on F5 joint walls and shows that they propagated as extension fractures. Abundant terminations of F5 joints against members of the F1, F2, and F3 sets underscore the relatively young age of this set; numerous examples were documented at more than 1/3 of the outcrops studied. Suggestion that the F5 set is younger than the F4 set, however, is based only on indirect evidence: at station no. 1, one of only two localities where these sets coexist, the F5 joints are absent from those parts of the outcrop where the F4 set is best expressed. Suppression of one joint set by the presence of another not far removed from it in strike (30° at this locality) is a common effect among extension joints but cannot often be used as a reliable discriminator of relative age.

The style of the F5 joint set is strongly dependent on the previous fracture history of the rock. Where older joints are abundant the F5 joints typically are short, subplanar in shape, and few in number. Where older sets are absent, however, and the F5 joints were the first set to form, they are present in great numbers as large, planar, visually prominent fractures much like those of the early F1 and F2 sets. This too is a common effect among extension joints and necessitates care in the use of joint style in correlating sets from one locality to another.

F5 joint surfaces exhibit moderate to locally heavy limonite staining and in some places are dotted with tiny (0.5-2 mm), cube-shaped pseudomorphs of limonite after pyrite. Diffusion bands of limonite impregnate the wall rock for distances of 2-5 cm from F5 joints at several localities. Fillings 1-3 mm thick of limonite-cemented sand were observed within F5 joints in the same roadcut (sta. no. 11) where similar material fills joints of the F1 set. Calcite coating F5 joint walls was observed at several localities and is of later deposition than the limonite; so too are the tiny, botryoidal aggregates of a translucent mineral resembling opal at station 11. The seemingly greater diversity of fracture-filling minerals in F5 joints relative to those of other sets probably is an artifact of their great numbers; further studies of older sets doubtless would reveal more of their mineralization history than that reported here.

F6 set: N. 25°-45° W. The F6 joint set is a minor one on the Rawlins uplift and is well expressed at only 1/7 of the stations studied. Orientations of the F6 joints overlap those of the much older F2 set (table 2), but abundant and clear abutting relations of F6 against F5 joints at three localities amply demonstrate the young age of the F6 set. Plumose structure on some F6 joint surfaces indicates they are extension joints.

Joints of the F6 set, like those of the earlier F5 set, differ in style depending in part on what joints were already present at the time of the F6 fracture episode. In the four outcrops where the F6 set is well developed, for example, it is one of only two sets present. The F6 set, however, is barely recognizable or is absent at all other localities where two or more older sets had formed. Spacings thus vary widely, from 2-10 cm (sta. 40) to many meters, but spacings of 1-3 m are the norm at three of the five localities where the set was recognized. The lengths of F6 joints are equally variable because of their tendency to terminate against whatever earlier joints were present; the small (20-50 cm long) F6 joints at station 40, for example, are wholly unlike the large (as much as 5 m long) F6 joints at station 17. Such widely varying properties are characteristic of young joint sets in complexly fractured areas.

The F6 joint surfaces in some places are limonite-stained, but generally not to the same degree as those of the F5 set in the same outcrops. Coatings of calcite were not observed on F6 joints.

F7 set: N. 55°-65° W. Joints of this late set on the Rawlins uplift are present in only two outcrops studied (table 2), in fine-grained sandstones in the lower part of the Upper Cretaceous section. At both localities they terminate against joints of the F5 set and are the youngest fractures present. They are similar in most respects to joints of the F6 set but have not yet been found with them; their identity as the youngest set thus is somewhat conjectural and is based principally on correlation to a similar set of known relative age on the Rock Springs uplift farther west. Surfaces of the F7 joints are lightly limonite-stained or not at all and at one locality (sta. 14) are coated with thin films of amber calcite.

JOINT SETS, ROCK SPRINGS UPLIFT

Twenty-one stations were established in Upper Cretaceous sandstones on the Rock Springs uplift (fig. 3), 19 in Mesaverde Group sandstone and two (fig. 3, sta. nos. 18 and 20) in the younger Fox Hills Sandstone. Six sets of joints, here designated Fa through Ff (table 4), were documented in this area; their possible correlation to sets on the Rawlins uplift farther east is discussed in a later section.

As on the Rawlins uplift, no outcrop observed on the Rock Springs uplift contains all six joint sets; most contain only two sets, and a few contain three (table 3). Opportunity to document relative ages among coexisting sets thus was limited at each outcrop studied by the small number of sets present, and for two sets their exact placement in the fracture sequence is uncertain. Field-observed properties of the joints in each set are fairly consistent from place to place within similar rock types throughout the stratigraphic section, but these properties differ markedly from one rock type to another, especially in response to variations in degree of cementation. Previous fracture history also exerted a strong influence on the character of later sets, as described below.

Fa set: N. 30°-40° W. Joints of the Fa set, the earliest set recognized on the Rock Springs uplift, were documented at more than 2/5 of the outcrops studied (table 3) and at all of them are the longest, most nearly planar, and most visually prominent joints present. The set is best developed in thinly bedded, firmly indurated, very fine grained sandstone beds interlayered with thick sequences of sandy shale in the Almond and Blair Formations, and also in a similar sandstone horizon near the base of the Rock Springs Formation.

The Fa joints are limonite-stained and cemented with calcite. On pavement exposures the joints commonly weather out as ridges, some as much as 1 cm wide, due to enhanced cementation of the wall rock by fluids circulating through the joints. Surface features indicative of extensile failure are common: delicately shaped arrest lines and plumose structures are exposed beneath the calcite fillings of many joints, and sharply formed twist-hackle fringes along the top and base of Fa joints were noted at several localities. Narrow zones of overlapping, closely spaced Fa joints are not uncommon and appear from a distance to be single, calcite-filled fractures of extraordinary length.

Fb set: N. 55°-65° W. Joints of the Fb set were found at only three localities on the Rock Springs uplift (table 3), all in well-cemented, very fine grained sandstones of the Almond and Rock Springs Formations. Their age relative to the Fa set is uncertain because the two sets were nowhere found to coexist. We have listed the Fb set as younger only because of its subordinate expression, a questionable criterion at best.

Joints of the Fb set, though seemingly sparsely distributed on the Rock Springs uplift, nevertheless are superbly developed wherever we have found them. Most are large, visually prominent fractures, commonly more than 2 m high and 5 m long, whose broad surfaces are either planar or undulate only gently along strike. Plumose structure, twist hackle, and arrest lines are common features. Zones of overlapping Fb joints, 5-20 cm wide and containing 3-10 joints along much of their length, were noted in several places, particularly within weakly cemented sandstone beds. Limonite forms dense coatings on many Fb joints and impregnates the adjacent wall rock for distances of 0.5-5 cm; the additional cement locally causes the joints to weather out in relief. Calcite, of later formation than the limonite, locally further cemented the wall rock and is preserved as small white patches on the faces of some Fb joints. A third mineral, probably barite, was observed at one locality as flattened rosettes of radiating crystals (sta. no. 31) on the faces of several Fb joints. In all these characteristics, save for details of mineralization, the Fb joints much resemble those of the more common Fa set.

Fc set: N. 20°-45° E. Joints of the Fc set occur at all stratigraphic levels within the Upper Cretaceous sandstones and are present in more than 3/5 of the outcrops studied on the Rock Springs uplift (table 3). In half of these they are the second-oldest set and form a crude set of subplanar cross joints with respect to the earlier Fa or Fb joints. Most Fc joints in such places terminate against the older joints and thus have lengths delimited by the spacings between them; lengths of only 0.5-2 m are typical. Where the older sets are absent and growth of the Fc joints was unconstrained, however, the Fc joints tend to be much longer (exposed lengths of 5 m or more are common), more nearly planar in shape, and in some places more abundant.

Walls of Fc joints are variably stained by limonite, in some places only lightly but in others so thoroughly that the rock is stained dark brown to nearly black. Impregnation of the adjacent wallrock by limonite is likewise common, locally in the form of diffusion bands extending up to 8 cm from each joint surface. Calcite is present on some Fc joints as white films and, like limonite, has indurated the joint walls so that Fc joints commonly weather into relief on pavement surfaces. Surface structures on Fc joints include arrest lines, twist hackle, and plumose structure, all common. Some Fc joints also show well-defined hooks into other Fc joints where these are closely spaced.

Fd set: N. 60°-80° E. Joints of the Fd set are among the most common joints on the Rock Springs uplift and are present at more than 1/3 (8 of 21) of the localities studied in detail (table 3). At three of these localities they form a set of cross joints with respect to the older Fa set; at four other localities none of the older sets are present and the Fd joints were the first to form. As with some of the other sets already discussed, the style of the Fd set is strongly linked to the previous fracture history of the rock.

The Fd joints form a visually prominent and superbly developed set in those places where they were the earliest joints to form. Typically they are very large fractures, among the largest on the uplift: exposed (partial) lengths of 5-7 m are common, and many are suspected of being considerably longer but cannot be traced throughout their full extent because of outcrop limitations. These large Fd joints are nearly planar or show only gentle sinuosity along strike except near their extremities, where some of them abruptly hook into adjacent members of the same set. In other areas where older Fa joints were already present, however, the Fd joints are of far different character. In shape, for example, they are notably more irregular and crudely formed; few are planar. Most are short, in some places only 30-45 cm long, because the pre-existing Fa joints presented effective barriers to fracture propagation. Many Fd joints terminate at both ends against the much-longer Fa joints. Long Fd joints in such places are the exception rather than the rule, but some cut across several Fa joints in succession and attain lengths as much as 3 m.

Limonite is common on Fd joints, locally as a light stain but more commonly as a dense precipitate that colors the joint walls dark brown and cements the adjacent rock. Diffusion bands parallel to the joint walls and extending as much as 8 cm into the rock were noted at one locality; they much resemble those associated with Fc joints. Calcite, though not commonly preserved on Fd joints, is present on some of them as coatings as much as 2 mm thick. Large, coarse plumose structure, arrest lines, and twist hackle are present on many Fd surfaces beneath the mineral fillings.

The age of the Fd joints relative to the Fc joints is uncertain. Though both sets are common, to date we have found them together at only a single locality. Even there, however, they occupy different parts of the outcrop, and no abutting relations were observed. Though the presence of the one set obviously inhibited development of the other--a common effect among joints not much different in strike--there is nothing in this relationship to indicate which set is the older of the two. In tables 3 and 4 the Fd set is provisionally listed as older than the Fc set based on analogy to the known relative ages of two sets of cleat in Cretaceous coals in the same area (Tyler and others, in press).

Fe set: N. 20°-45° W. Joints of the Fe set are present in only six of the outcrops studied (table 3), generally as a set of cross joints that terminate laterally against members of the Fc set (two localities) or Fd set (three localities). Most Fe joints thus are of only modest length, commonly 1-3 m, but some attain lengths of 5-6 m in those parts of the outcrops where the older joints are sparse. At the single locality where Fe joints were the first to form--in a thick, poorly indurated sandstone of the Rock Springs Formation (sta. no. 42)--they are longer still, 3-10 m. The shapes of Fe joints are as variable as their size and range from subplanar (and commonly undulatory along strike) where older joints are abundant, to nearly planar where the older fractures are sparse to absent. Surface structures, including arrest lines, twist hackle, plumose structure, and also hooks of Fe joints against other Fe joints, are common at most localities. Limonite coats many Fe joints and cements the adjacent wall rock, but generally to a much lesser extent than is common among the older joints. Most Fe surfaces are stained only pale orange to medium brown. Calcite, in remnant patches as much as 2 mm thick, was noted on Fe joints at only one locality (sta. no. 33).

Ff set: N. 55°-85° W. Joints of this late and sparsely distributed set (table 3) exhibit all the expected characteristics of a late-formed set in a complexly fractured area. Almost invariably they are short--commonly only 10-50 cm--because they terminate against whatever older fractures are present; it is only where the older joints are widely spaced (or a rare Ff joint cuts across them) that some members of the Ff set attain lengths of 1-2 m. The Ff joints, more so than those of any other set, are irregular in shape. Nearly all curve perceptibly, some markedly, along both strike and dip, and some split along bedding surfaces partway along their length to form two subsidiary fractures of lesser height. Mineral coatings are almost wholly lacking on Ff joints except at one locality, where several joints are lightly limonite-stained. Proof of their young age is shown by terminations of Ff joints against members of the Fe set at the single locality where the two sets coexist.

DISCUSSION

Correlation of Joint Sets Between Uplifts

Median strikes and possible correlations between joint sets on the Rawlins and Rock Springs uplifts are shown in table 4. Some observations:

(a) The F1 joint set, a particularly well expressed set on the Rawlins uplift, is missing from the Rock Springs area. The fracture history of the Upper Cretaceous rocks along the east side of the Washakie basin began before that of correlative rocks 100 km farther west.

(b) Of the six remaining joint sets found on the Rawlins uplift, five of them have probable counterparts on the Rock Springs uplift; the sets in both areas have comparable orientations and formed in the same sequence. Though of regional extent, most sets differ markedly in prominence from one uplift to the other. Only one joint set, the F5-Fd set, is a major set on both uplifts. The differing prominence from one area to another is a common feature of regional joint sets and is hardly surprising in view of the distances involved.

(c) The strong fracture event recorded by the prominent Fc joint set on the Rock Springs uplift did not result in joint formation on the Rawlins uplift.

Thus, of the thirteen total sets identified, ten of them can be matched between the two areas to define five regional joint events. The remaining three sets appear to be unique to one uplift or the other. These latter are of particular interest in defining differences in tectonic history between the two uplifts, but interpretation of their significance must await work in younger units to establish upper bounds on the age of each fracture set.

CONCLUSIONS

Upper Cretaceous sandstones bordering the Washakie basin in southern Wyoming are cut by a complex network of extension joints. Preliminary interpretation of fracture data from the Rawlins uplift along the eastern basin margin suggests that seven episodes of fracture affected these rocks. Six sets of joints cut correlative strata on the Rock Springs uplift along the western basin margin 100 km distant. The earliest set of joints is missing from the Rock Springs area, showing that brittle deformation of the Cretaceous strata began earlier in the eastern part of the basin than farther west. Most of the later joint sets, however, can be matched from one uplift to the other to define five episodes of fracture of regional extent. All but the youngest joints at each locality are nearly perpendicular to bedding, regardless of present bed dip, showing that most of the joint sets predate the final phases of tilting along the basin margins.

The character of the fracture network shows wide variation from one locality to another and even within different beds at the same outcrop, but much of the variation is systematic. For any given joint set, the three factors that most affect several key joint properties (length, height, spacing, shape) are lithology (particularly degree of cementation), bed thickness, and previous joint history. Stratigraphic position within the Upper Cretaceous section had only a minimal effect; we have noted no major changes in the overall fracture network from the base of the Mesaverde Group to the top of the Fox Hills Sandstone. The close correlation between fracture style and lithology, and the similarity in fracture history between the two uplifts, suggest that several properties of the fracture network in correlative reservoir strata beneath the intervening basin are potentially predictable from detailed outcrop studies.

The sequence in which the sets formed (table 4) is potentially interpretable in terms of a counterclockwise rotation of the stress field over time. At present, however, we know only the relative but not the absolute ages of the joint sets and thus lack information on which sets are related genetically across the basin. Tracing of the fracture network upward through the Tertiary basin strata will be necessary to interpret the fracture history in terms of the tectonic and paleostress evolution of the region. A continuous record of post-Laramide counterclockwise stress rotation through an angle of at least 60°, however, has been documented for other areas to the south, including the Piceance basin (Verbeek and Grout, 1986), the Uinta basin (Verbeek and Grout, 1992), and the Paradox basin (Grout and Verbeek, in press).

ACKNOWLEDGMENTS.–This work was supported by the U.S. Geological Survey Tight Gas Sands and National Cooperative Geologic Mapping Programs. We thank R.C. Surdam and Cheryl Jaworowski, both of the University of Wyoming, for their timely review. Christy Jones and R.E. Sabala drafted the figures.

REFERENCES CITED

Bader, J.B., 1987, Surface and subsurface structural relations of the Cherokee Ridge arch, south-central Wyoming: San Jose, California, San Jose State University unpublished M.S. thesis, 68 p.

______ 1990, Subsurface correlations of Upper Cretaceous and Tertiary rocks, southern Washakie basin, Colorado: U.S. Geological Survey Open-File Report 90-325, 2 sheets.

Bader, J.B., Gill, J.R., Cobban, W.A., and Law, B.E., 1983, Biostratigraphic correlation chart of some Upper Cretaceous rocks from the Lost Soldier area, Wyoming to west of Craig, Colorado: U.S. Geological Survey Miscellaneous Field Studies Map MF-1548, 1 sheet.

Brown, W.G., 1988, Deformational style of Laramide uplifts in the Wyoming foreland, in Schmidt, C.J., and Perry, W.J., Jr., eds., Interaction of the Rocky Mountain foreland and the Cordilleran thrust belt: Geological Society of America Memoir 171, p. 1-25.

Gries, Robbie, 1983, North-south compression of Rocky Mountain foreland structures, in Lowell, J.D., ed., Rocky Mountain foreland basins and uplifts: Rocky Mountain Association of Geologists, p. 9-32.

Grout, M.A., and Verbeek, E.R., 1983, Field studies of joints--Insufficiencies and solutions, with examples from the Piceance basin, Colorado, in Gary, J.H., ed., 16th Oil Shale Symposium, Proceedings: Golden, Colorado School of Mines Press, p. 68-80.

______ in press, Regional joint sets are genetically unrelated to anticlinal structures, northern Paradox basin, southeastern Utah and southwestern Colorado, in Friedman, J.D., and Huffman, A.C., Jr., eds., Laccolith complexes of southeastern Utah--Tectonic control and time of emplacement: U.S. Geological Survey Bulletin.

Guth, P.L., 1987, MicroNET (computer software): Petmar Trilobite Breeding Ranch, University of Nevada at Las Vegas, version 1.0.

Hamilton, W.B., 1988, Laramide crustal shortening, in Schmidt, C.J., and Perry, W.J., Jr., eds., Interaction of the Rocky Mountain foreland and the Cordilleran thrust belt: Geological Society of America Memoir 171, p. 27-39.

Hettinger, R.D., and Kirschbaum, M.A., 1991, Chart showing correlations of some Upper Cretaceous and lower Tertiary rocks, from the east flank of the Washakie basin to the east flank of the Rock Springs uplift, Wyoming: U.S. Geological Survey Miscellaneous Investigations Series Map I-2152, 1 sheet.

Hettinger, R.D., Honey, J.G., and Nichols, D.J., 1991, Chart showing correlations of Upper Cretaceous Fox Hills Sandstone and Lance Formation, and lower Tertiary Fort Union, Wasatch, and Green River Formations, from the eastern flank of the Washakie basin to the southeastern part of the

Great Divide basin, Wyoming: U.S. Geological Survey Miscellaneous Investigations Series Map I-2151, 1 sheet.

Kauffman, E.G., 1985, Cretaceous evolution of the Western Interior basin of the United States, in Pratt, L.M., Kauffman, E.G., and Zelt, F.B., eds., Fine-grained deposits and biofacies of the Cretaceous Western Interior seaway—Evidence of cyclic sedimentation processes: Society of Economic Paleontologists and Mineralogists Guidebook No. 4, p. IV-XIII.

Kulander, B.R., Barton, C.C., and Dean, S.L., 1979, The application of fractography to core and outcrop fracture investigations: United States Department of Energy, Report METC/SP-79-3, 174 p.

Lickus, M.R., and Law, B.E., 1988, Structure contour map of the Greater Green River basin, Wyoming, Colorado, and Utah: U.S. Geological Survey Miscellaneous Field Studies Map MF-2031, scale 1:500,000.

Love, J.D., and Christiansen, A.C., 1985, Geologic map of Wyoming: U.S. Geological Survey Map, scale 1:500,000, 3 sheets.

McDonald, R.E., 1975, Structure, correlation and depositional environments of the Tertiary Sand Wash and Washakie basins, Colorado and Wyoming, in Bolyard, D.W., ed., Deep drilling frontiers of the central Rocky Mountains: Rocky Mountain Association of Geologists, p. 175-184.

Pollard, D.D., and Aydin, Atilla, 1988, Progress in understanding jointing over the past century: Geological Society of America Bulletin, v. 100, no. 8, p. 1181-1204.

Roehler, H.W., 1985, Geologic map of the Kinney Rim 30 x 60 minute quadrangle, Wyoming and Colorado: U.S. Geological Survey Miscellaneous Investigations Series Map I-1615, scale 1:100,000.

Stearns, D.W., 1978, Faulting and forced folding in the Rocky Mountain foreland, in Matthews, Vincent, III, ed., Laramide folding associated with basement block faulting in the western United States: Geological Society of America Memoir 151, p. 1-37.

Tyler, Roger, Laubach, S.E., Ambrose, W.A., Tremain, C.M., and Grout, M.A., in press, Coal fracture patterns in the foreland of the Cordilleran thrust belt, western United States: The 1993 International Coalbed Methane Symposium, May 17-21, 1993, Birmingham, Alabama.

Verbeek, E.R., and Grout, M.A., 1986, Cenozoic stress rotation, northeastern Colorado Plateau, in Stone, D.S., ed., New interpretations of northwest Colorado geology: Rocky Mountain Association of Geologists, p. 97.

______ 1992, Structural evolution of gilsonite dikes, eastern Uinta basin, Utah, in Fouch, T.D., Nuccio, V.F., and Chidsey, T.C., Jr., eds., Hydrocarbon and mineral resources of the Uinta basin, Utah and Colorado: Utah Geological Association Guidebook 20, p. 237-255.

APPENDIX: JOINT-ORIENTATION DATA. Joint-orientation data (unrotated) collected at each locality (station) in the Upper Cretaceous sandstones on the Rawlins and Rock Springs uplifts, Washakie basin, are depicted on Schmidt lower hemisphere equal-area plots using the MicroNET program of Guth (1987). Each plot contains joint data from one station and has been given an identification number according to the sequence in which data were collected. These numbers correspond to the station numbers on the maps of the study area (figs. 2, 3). The orientation data also are tabulated by joint set (table 4) and listed below each equal-area plot. Bedding attitudes (So) also are listed.

STATION WB-1

n = 69

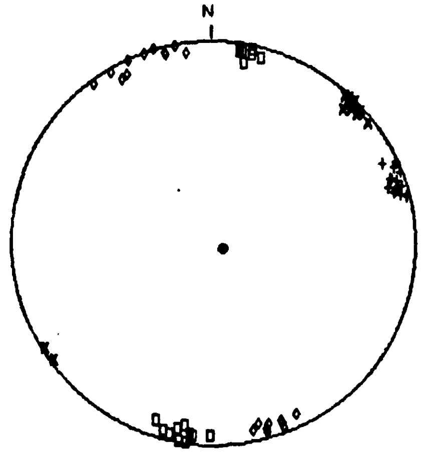

- + WB1F2 n = 15
- x WB1F3 n = 13
- ▫ WB1F4 n = 17
- ◊ WB1F5 n = 21
- • WB1SO n = 3

Schmidt net, lower hemisphere projection

WB1F2	WB1F3	WB1F4	WB1F5	WB1SO
N16W82SW	N46W87SW	N79W83NE	N73E90SE	N27E05NW
N17W87SW	N42W88SW	N80W80SW	N82E85SE	N20E04NW
N21W89SW	N42W85SW	N78W85SW	N76E87SE	N36E05NW
N18W80SW	N46W82SW	N75W84SW	N69E84NW	
N19W85SW	N44W85SW	N84W85NE	N76E86SE	
N20W82SW	N48W88SW	N75W85NE	N59E88SE	
N14W88SW	N42W87SW	N89W85NE	N76E81NW	
N25W82SW	N45W90SW	N83W87NE	N74E87NW	
N15W85SW	N47W89SW	N83W84NE	N61E82SE	
N24W89SW	N38W87SW	N82W89NE	N74E85NW	
N17W84SW	N36W88NE	N80W89NE	N73E83NW	
N20W83SW	N45W87SW	N82W86SW	N63E83SE	
N16W83SW	N32W89NE	N81W80NE	N64E83NW	
N17W85SW		N78W88SW	N53E88SE	
N23W87SW		N81W86SW	N69E87NW	
		N72W81NE	N69E83NW	
		N77W86NE	N69E84NW	
			N79E89SE	
			N78E84NW	
			N70E89SE	
			N65E89SE	

STATION WB-2

n = 40

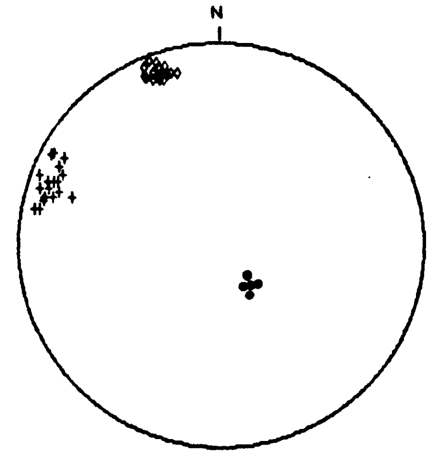

- + WB2F1 n = 18
- ◊ WB2F5 n = 17
- • WB2SO n = 5

Schmidt net, lower hemisphere projection

WB2F1	WB2F5	WB2SO
N17E83SE	N70E78SE	N60E23NW
N24E74SE	N68E77SE	N48E16NW
N16E75SE	N73E82SE	N61E19NW
N14E79SE	N69E80SE	N53E20NW
N21E75SE	N71E78SE	N45E21NW
N11E80SE	N66E79SE	
N21E77SE	N67E85SE	
N11E83SE	N69E87SE	
N29E83SE	N76E77SE	
N18E78SE	N66E80SE	
N29E77SE	N73E77SE	
N18E73SE	N71E82SE	
N18E66SE	N73E78SE	
N28E84SE	N74E77SE	
N20E80SE	N71E85SE	
N26E77SE	N71E75SE	
N15E79SE	N70E76SE	
N21E85SE		

STATION WB-3

n = 35

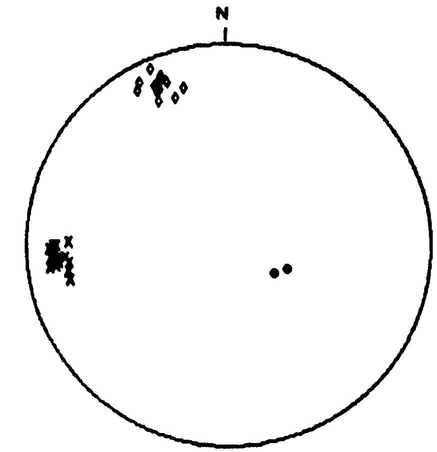

- x WB3F2 n = 18
- ◊ WB3F5 n = 15
- • WB3SO n = 2

Schmidt net, lower hemisphere projection

WB3F2	WB3F5	WB3SO
N01W78NE	N67E85SE	N22E26NW
N12W69NE	N71E66SE	N33E22NW
N02W75NE	N60E77SE	
N04W70NE	N66E72SE	
N00W76NE	N68E77SE	
N09W69NE	N70E75SE	
N05W75NE	N62E81SE	
N05W74NE	N66E76SE	
N06W68NE	N67E73SE	
N06W73NE	N70E76SE	
N04W77NE	N69E79SE	
N05W74NE	N67E75SE	
N07W78NE	N75E70SE	
N06W73NE	N62E81SE	
N04W73NE	N65E68SE	
N07W75NE		
N01E68SE		
N00W74NE		

STATION WB-4

n = 39

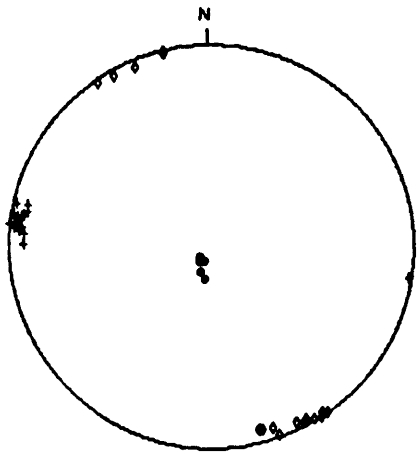

+	WB4F1	n =	18
◊	WB4F5	n =	16
•	WB4SO	n =	5

Schmidt net, lower hemisphere projection

WB4F1	WB4F5	WB4SO
N01E82SE	N57E88NW	N66W11NE
N13E82SE	N56E90NW	N77W13NE
N09E84SE	N63E88NW	N67W07NE
N11E81SE	N56E88SE	N44W06NE
N13E88SE	N62E87NW	N54W08NE
N07E87SE	N61E87SE	
N06E83SE	N65E86NW	
N10E89NW	N60E89NW	
N10E89SE	N77E89SE	
N05E85SE	N77E88SE	
N04E82SE	N58E90NW	
N08E84SE	N68E86SE	
N09E86SE	N72E84NW	
N07E90SE	N71E89NW	
N08E86SE	N76E83NW	
N06E88SE	N75E83NW	
N10E83SE		
N09E84SE		

STATION WB-5

n = 30

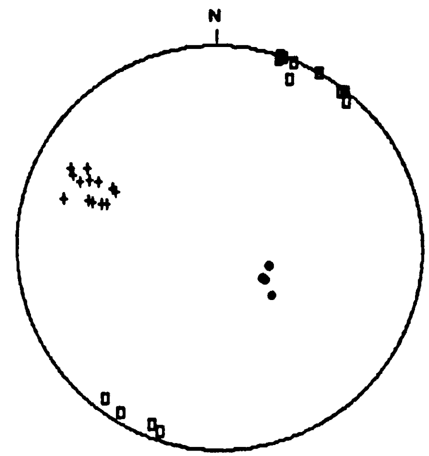

+	WB5F1	n =	13
▪	WB5F3	n =	13
•	WB5SO	n =	4

Schmidt net, lower hemisphere projection

WB5F1	WB5F3	WB5SO
N21E50SE	N60W90SW	N35E23NW
N31E65SE	N68W89SW	N42E29NW
N28E48SE	N67W80SW	N35E22NW
N19E58SE	N59W85NE	N20E22NW
N27E61SE	N72W88SW	
N26E69SE	N72W85NE	
N28E72SE	N52W88SW	
N19E56SE	N71W90SW	
N29E50SE	N49W86SW	
N20E52SE	N53W83NE	
N28E57SE	N51W89SW	
N17E69SE	N72W90SW	
N25E65SE	N69W83NE	

STATION WB-6

n = 31

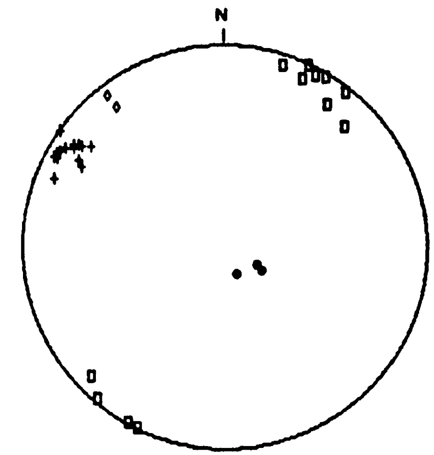

+	WB6F1	n =	14
▪	WB6F3	n =	12
◊	WB6F5	n =	2
•	WB6SO	n =	3

Schmidt net, lower hemisphere projection

WB6F1	WB6F3	WB6F5	WB6SO
N35E75SE	N65W89SW	N52E76SE	N28E15NW
N28E83SE	N50W88NE	N52E84SE	N65E12NW
N32E82SE	N61W89NE		N32E18NW
N28E85SE	N64W89NE		
N37E72SE	N45W73SW		
N22E80SE	N62W86SW		
N34E79SE	N72W84SW		
N31E73SE	N44W81NE		
N33E78SE	N65W81SW		
N35E89SE	N59W88SW		
N30E83SE	N54W76SW		
N29E70SE	N52W87SW		
N29E84SE			
N35E77SE			

STATION WB-7

n = 20

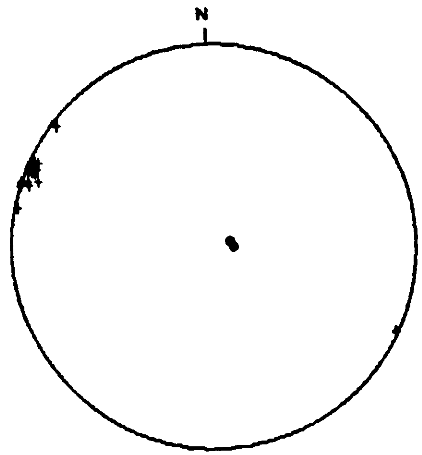

+	WB7F1	n =	18
●	WB7SO	n =	2

Schmidt net, lower hemisphere projection

WB7F1	WB7SO
N20E90SE	N02W08SW
N24E85SE	N15W07SW
N24E87SE	
N20E86SE	
N39E87SE	
N27E88SE	
N19E90SE	
N26E89SE	
N25E85SE	
N24E86SE	
N21E87SE	
N27E89NW	
N22E82SE	
N25E89SE	
N13E89SE	
N27E85SE	
N24E89SE	
N24E85SE	

STATION WB-8

n = 36

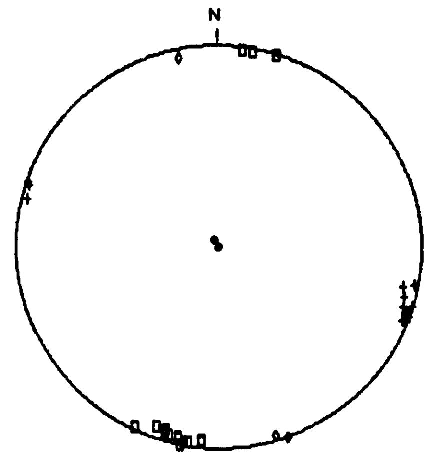

+	WB8F1	n =	16
■	WB8F4	n =	15
◊	WB8F5	n =	3
●	WB8SO	n =	2

Schmidt net, lower hemisphere projection

WB8F1	WB8F4	WB8F5	WB8SO
N14E87SE	N80W88NE	N73E87NW	N00E00SE
N12E82NW	N79W90NE	N78E85SE	N55E03SE
N15E84NW	N78W87NE	N70E90NW	
N19E87NW	N73W89SW		
N17E90NW	N78W86NE		
N19E89SE	N75W86NE		
N22E87NW	N85W87NE		
N19E89NW	N85W86NE		
N19E89NW	N80W88SW		
N11E88NW	N74W84NE		
N20E90NW	N71W84NE		
N19E88NW	N65W88NE		
N18E85NW	N81W88NE		
N20E88NW	N83W88SW		
N18E88SE	N74W86NE		
N22E89NW			

STATION WB-9

n = 39

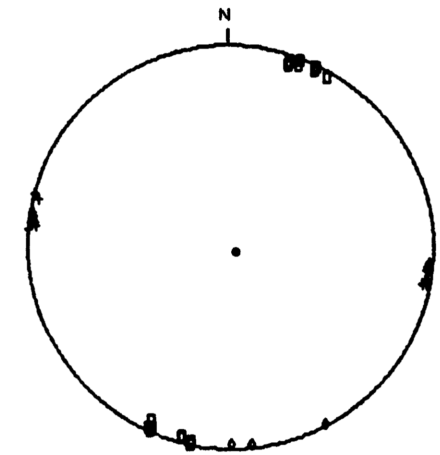

+	WB9F1	n =	19
■	WB9F3	n =	16
◊	WB9F5	n =	3
●	WB9SO	n =	1

Schmidt net, lower hemisphere projection

WB9F1	WB9F3	WB9F5	WB9SO
N11E88NW	N78W88NE	N62E89NW	N35E03NW
N07E89SE	N75W86NE	N84E88NW	
N10E88NW	N69W89SW	N90E87NW	
N10E89SE	N72W84SW		
N06E86SE	N65W88NE		
N11E86NW	N65W84NE		
N09E88SE	N66W89NE		
N05E90SE	N72W86SW		
N14E87SE	N75W87NE		
N07E87NW	N69W86SW		
N08E89SE	N66W88NE		
N10E87NW	N66W87NE		
N05E88NW	N60W87SW		
N07E88NW	N78W90NE		
N07E87SE	N64W89SW		
N15E90SE	N64W87SW		
N06E87NW			
N09E88SE			
N08E88SE			

STATION WB-10

n = 31

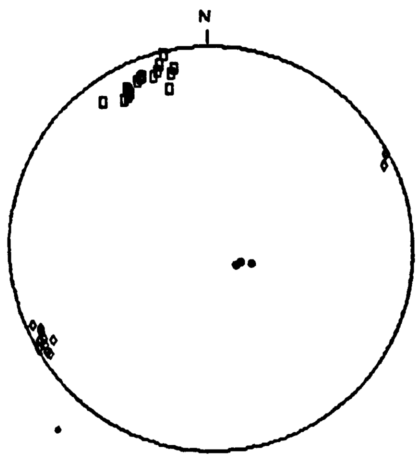

▪ WB10F5	n =	16
◊ WB10F6	n =	12
• WB10SO	n =	3

Schmidt net, lower hemisphere projection

WB10F5	WB10F6	WB10SO
N63E77SE	N32W86NE	N26E13NW
N74E80SE	N28W89SW	N21E17NW
N68E80SE	N33W85NE	N36E12NW
N79E80SE	N25W85SW	
N77E88SE	N28W86NE	
N75E83SE	N30W80NE	
N54E78SE	N25W83NE	
N69E80SE	N30W85NE	
N76E70SE	N26W84NE	
N60E73SE	N30W89NE	
N78E78SE	N23W86NE	
N67E79SE	N28W84NE	
N63E78SE		
N72E78SE		
N63E75SE		
N62E74SE		

STATION WB-11

n = 30

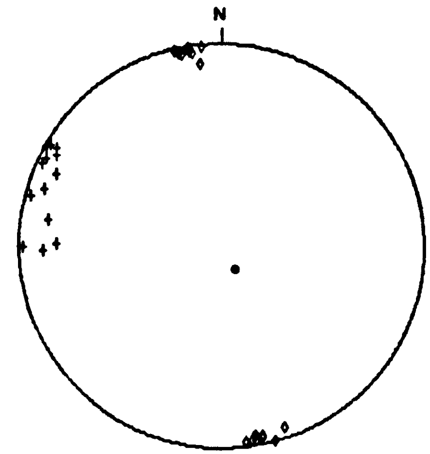

♦ WB11F1	n =	13
◊ WB11F5	n =	16
• WB11SO	n =	1

Schmidt net, lower hemisphere projection

WB11F1	WB11F5	WB11SO
N02W77NE	N80E87SE	N55E11NW
N23E78SE	N79E87NW	
N00W70NE	N70E84NW	
N26E86SE	N82E87NW	
N08E75SE	N77E85NW	
N30E84SE	N83E80SE	
N01W88NE	N74E90NW	
N30E88SE	N76E89SE	
N28E82SE	N80E89SE	
N29E89SE	N78E86SE	
N14E87SE	N77E86NW	
N17E81SE	N84E89SE	
N24E87SE	N80E87NW	
	N79E85NW	
	N77E87SE	
	N81E86SE	

STATION WB-12

n = 44

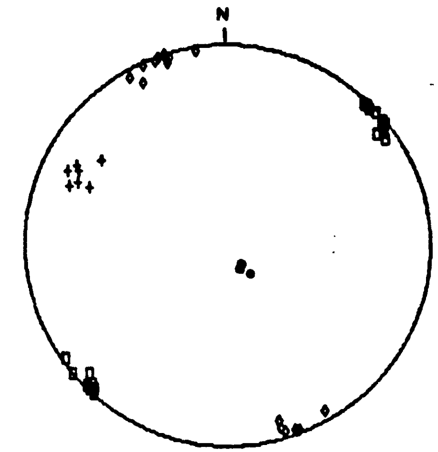

♦ WB12F1	n =	7
▪ WB12F3	n =	18
◊ WB12F5	n =	16
• WB12SO	n =	3

Schmidt net, lower hemisphere projection

WB12F1	WB12F3	WB12F5	WB12SO
N23E63SE	N40W90NE	N72E90SE	N50E15NW
N27E71SE	N46W88SW	N69E88SE	N51E10NW
N21E72SE	N46W89NE	N69E88NW	N61E11NW
N34E64SE	N34W84SW	N72E85SE	
N23E69SE	N39W89SW	N73E86NW	
N25E76SE	N35W88NE	N72E88SE	
N28E73SE	N45W88SW	N74E84NW	
	N43W83NE	N70E89SE	
	N42W89SW	N70E87NW	
	N44W88SW	N65E88SE	
	N47W87NE	N81E88SE	
	N37W82SW	N74E80NW	
	N38W87SW	N60E86SE	
	N46W86NE	N60E85NW	
	N36W86SW	N63E80SE	
	N38W89SW	N73E87SE	
	N45W88NE		
	N48W90NE		

STATION WB-13

n = 53

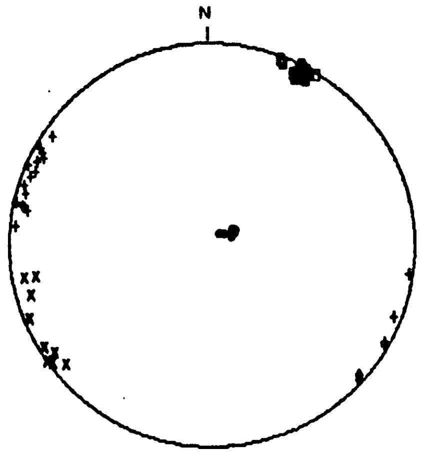

+	WB13F1	n =	19
x	WB13F2	n =	9
■	WB13F3	n =	17
◊	WB13F5	n =	2
●	WB13SO	n =	6

Schmidt net, lower hemisphere projection

WB13F1	WB13F2	WB13F3	WB13F5	WB13SO
N31E88NW	N22W87NE	N61W86SW	N43E88NW	N57W06SW
N18E87SE	N15W82NE	N61W84SW	N42E86NW	N40W07SW
N35E85SE	N10W83NE	N61W89SW		N36W10SW
N09E88NW	N10W77NE	N60W87SW		N28W10SW
N16E85SE	N31W87NE	N63W90SW		N33W11SW
N06E87SE	N34W84NE	N64W84SW		N22W09SW
N21E85SE	N39W83NE	N63W84SW		
N23E84SE	N35W90NE	N60W84SW		
N22E86NW	N36W88NE	N63W87SW		
N11E82SE		N62W89SW		
N29E85SE		N61W87SW		
N28E83SE		N63W82SW		
N24E89SE		N62W86SW		
N30E87SE		N68W87SW		
N12E84SE		N60W88SW		
N26E85SE		N69W88SW		
N12E85SE		N58W89SW		
N13E89SE				
N30E87NW				

STATION WB-14

n = 33

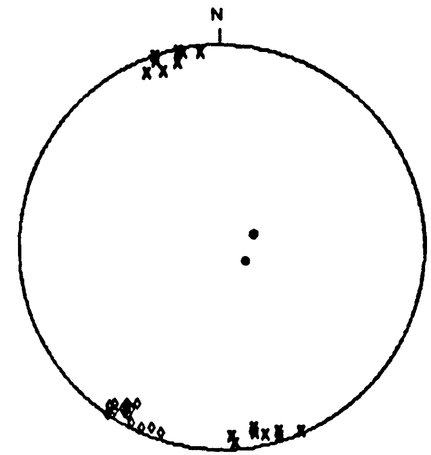

x	WB14F5	n =	16
◊	WB14F7	n =	15
●	WB14SO	n =	2

Schmidt net, lower hemisphere projection

WB14F5	WB14F7	WB14SO
N77E84NW	N69W85NE	N24W14SW
N78E89SE	N55W85NE	N30E11NW
N80E82NW	N66W87NE	
N67E83SE	N56W83NE	
N80E80NW	N72W86NE	
N73E84NW	N60W84NE	
N77E83SE	N59W79NE	
N71E90SE	N61W81NE	
N67E89NW	N62W77NE	
N73E87NW	N59W83NE	
N84E86SE	N63W87NE	
N87E83NW	N56W90NE	
N79E87SE	N61W84NE	
N72E80SE	N57W86NE	
N86E87NW	N60W82NE	
N71E87SE		

STATION WB-15

n = 34

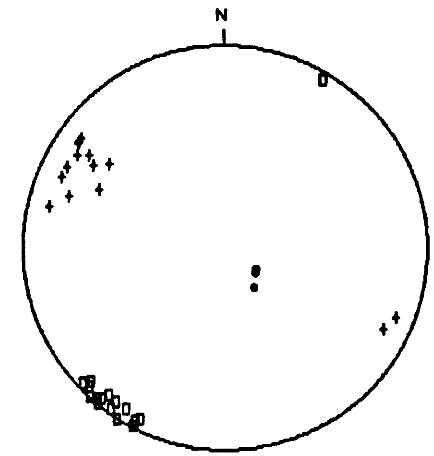

+	WB15F1	n =	14
■	WB15F3	n =	17
●	WB15SO	n =	3

Schmidt net, lower hemisphere projection

WB15F1	WB15F3	WB15SO
N32E75SE	N48W90NE	N33E15NW
N36E60SE	N63W86NE	N53E20NW
N23E77SE	N58W90NE	N38E16NW
N34E70SE	N55W83NE	
N25E58SE	N51W89NE	
N37E78SE	N50W88NE	
N13E78SE	N55W87NE	
N35E78SE	N44W87NE	
N18E70SE	N51W86NE	
N36E78SE	N60W86SW	
N27E77SE	N63W89NE	
N22E80NW	N45W83NE	
N32E66SE	N52W82NE	
N27E77NW	N64W84NE	
	N59W83NE	
	N50W87NE	
	N46W86NE	

STATION WB-16

n = 36

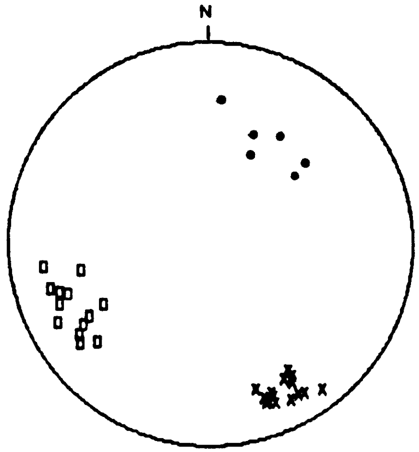

x WB16F5 n = 17
▪ WB16F6 n = 13
• WB16SO n = 6

Schmidt net, lower hemisphere projection

WB16F5	WB16F6	WB16SO
N53E80NW	N30W51NE	N68W49SW
N73E65NW	N28W74NE	N57W54SW
N71E73NW	N22W69NE	N39W45SW
N60E75NW	N18W67NE	N85W61SW
N68E71NW	N20W64NE	N65W41SW
N70E72NW	N38W70NE	N41W52SW
N60E68NW	N08W72NE	
N62E65NW	N35W68NE	
N63E76NW	N41W63NE	
N60E69NW	N33W64NE	
N59E66NW	N16W71NE	
N71E70NW	N31W59NE	
N59E63NW	N12W55NE	
N68E69NW		
N58E76NW		
N60E68NW		
N68E74NW		

STATION WB-17

n = 39

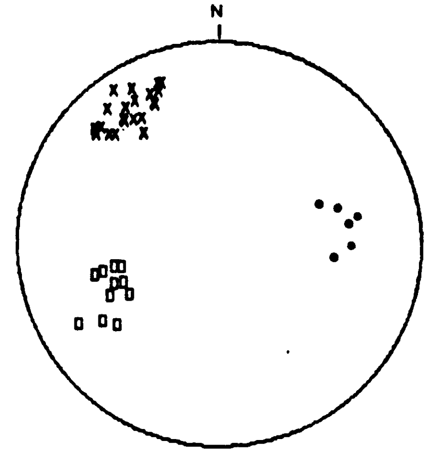

x WB17F5 n = 21
▪ WB17F6 n = 12
• WB17SO n = 6

Schmidt net, lower hemisphere projection

WB17F5	WB17F6	WB17SO
N70E73SE	N26W50NE	N22W44SW
N65E65SE	N21W46NE	N00E55SW
N46E63SE	N15W53NE	N06E48NW
N65E70SE	N30W69NE	N10W55SW
N42E72SE	N22W42NE	N12W59SW
N58E62SE	N34W58NE	N18W51SW
N55E81SE	N14W41NE	
N52E65SE	N13W44NE	
N55E55SE	N14W49NE	
N65E64SE	N30W42NE	
N55E70SE	N39W54NE	
N59E70SE	N30W42NE	
N44E70SE		
N50E75SE		
N68E70SE		
N69E73SE		
N44E65SE		
N52E66SE		
N55E63SE		
N60E76SE		
N41E70SE		

STATION WB-18

n = 29

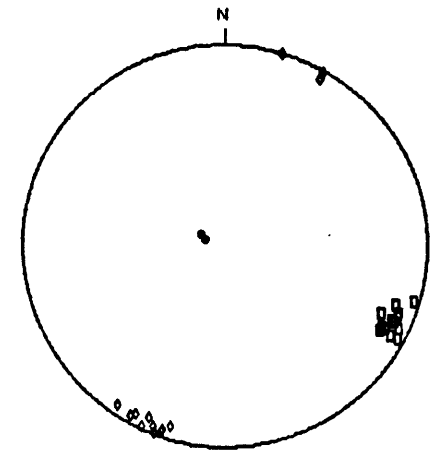

▪ FC n = 14
◊ FF n = 13
• SO n = 2

Schmidt net, lower hemisphere projection

WB18FC	WB18FF	WB18SO
N19E78NW	N72W86NE	N15E08SE
N27E76NW	N63W84NE	N23E10SE
N16E87NW	N62W86NE	
N24E79NW	N57W85NE	
N24E81NW	N72W87NE	
N28E82NW	N61W85SW	
N24E80NW	N74W90SW	
N27E78NW	N66W88NE	
N21E81NW	N74W83NE	
N28E86NW	N61W89SW	
N28E76NW	N67W83NE	
N22E81NW	N70W89NE	
N23E73NW	N69W86NE	
N25E84NW		

STATION WB-19

n = 33

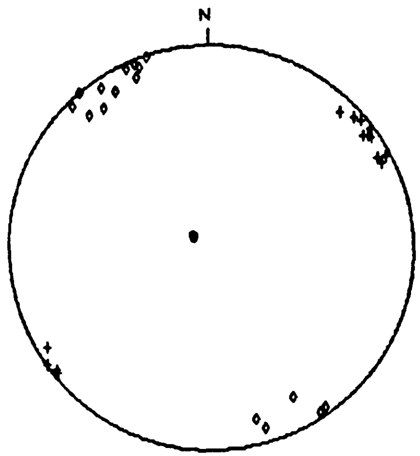

+	FA	n =	14
◊	FD	n =	16
•	SO	n =	3

Schmidt net, lower hemisphere projection

WB19FA	WB19FD	WB19SO
N36W88SW	N65E87SE	N33E08SE
N39W88NE	N57E87NW	N39E09SE
N36W83SW	N74E82NW	N39E08SE
N27W87SW	N68E88SE	
N46W82SW	N56E85SE	
N35W89NE	N76E77NW	
N34W86SW	N53E75SE	
N38W87NE	N50E90SE	
N35W85SW	N67E81SE	
N31W84NE	N59E79SE	
N42W85SW	N62E73NW	
N28W83SW	N55E86NW	
N40W87SW	N46E87SE	
N26W84SW	N72E89SE	
	N48E77SE	
	N69E85SE	

STATION WB-20

n = 27

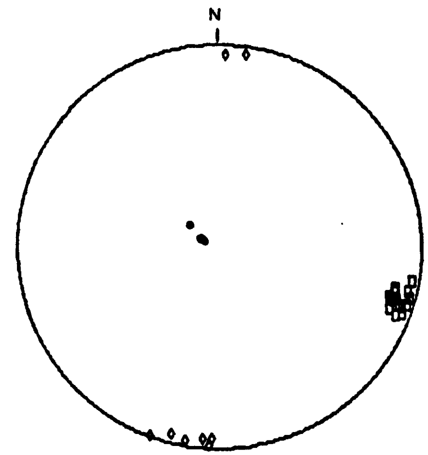

▪	FC	n =	14
◊	FF	n =	9
•	SO	n =	4

Schmidt net, lower hemisphere projection

WB20FC	WB20FF	WB20SO
N17E78NW	N82W86SW	N38E14SE
N18E82NW	N85W85NE	N31E07SE
N21E82NW	N88W85SW	N27E08SE
N20E78NW	N76W85NE	N28E06SE
N10E86NW	N88W85NE	
N13E85NW	N70W89NE	
N20E85NW	N88W85NE	
N15E87NW	N87W88NE	
N13E78NW	N80W87NE	
N16E80NW		
N17E86NW		
N14E78NW		
N18E84NW		
N16E76NW		

STATION WB-21

n = 39

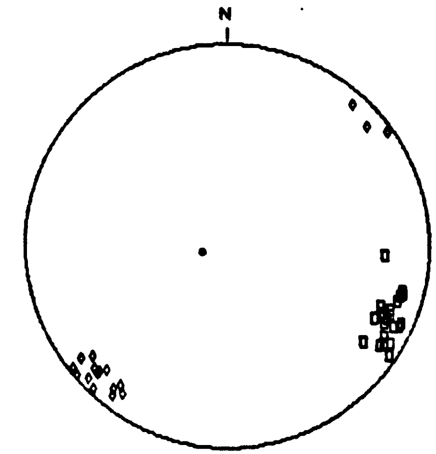

▪	FC	n =	21
◊	FE	n =	17
•	SO	n =	1

Schmidt net, lower hemisphere projection

WB21FC	WB21FE	WB21SO
N23E76NW	N53W83NE	N15W10NE
N35E71NW	N41W88NE	
N16E78NW	N52W80NE	
N24E83NW	N38W81NE	
N21E70NW	N55W79NE	
N34E86NW	N40W76NE	
N31E83NW	N47W87NE	
N26E70NW	N45W80NE	
N26E75NW	N53W76NE	
N33E79NW	N46W75NE	
N21E75NW	N43W79NE	
N26E80NW	N41W80SW	
N30E78NW	N49W83SW	
N25E83NW	N45W78NE	
N32E80NW	N36W87SW	
N03E67NW	N39W88NE	
N23E72NW	N44W85NE	
N14E78NW		
N15E79NW		
N24E75NW		
N18E77NW		

STATION WB-22
n = 16

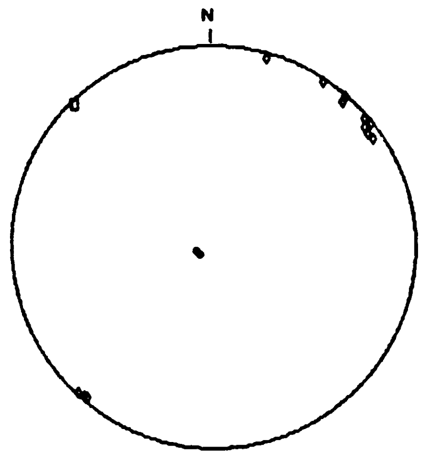

- FC n = 1
- FE n = 13
- SO n = 2

Schmidt net, lower hemisphere projection

WB22FC	WB22FE	WB22SO
N46E88SE	N48W89SW	N18W07NE
	N40W88SW	N32W07NE
	N47W89NE	
	N74W87SW	
	N50W88NE	
	N34W85SW	
	N56W88SW	
	N48W86SW	
	N49W88NE	
	N50W88NE	
	N38W85SW	
	N36W84SW	
	N38W89SW	

STATION WB-23
n = 29

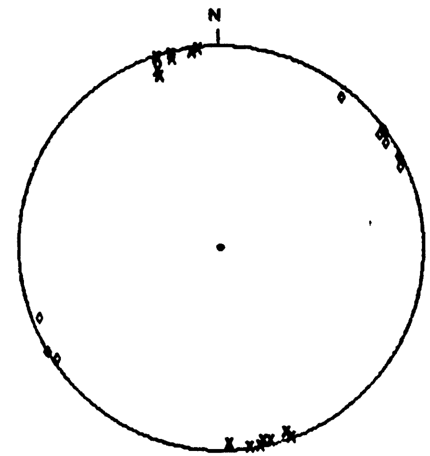

- FD n = 18
- FE n = 10
- SO n = 1

Schmidt net, lower hemisphere projection

WB23FD	WB23FE	WB23SO
N82E87SE	N35W86SW	N00E00SE
N72E89SE	N35W89SW	
N82E89NW	N32W86SW	
N70E89NW	N27W89SW	
N88E86NW	N51W85SW	
N76E89SE	N36W89SW	
N78E87NW	N24W87SW	
N76E86SE	N34W88NE	
N72E88SE	N31W90NE	
N84E89SE	N21W86NE	
N71E79SE		
N71E86NW		
N79E89NW		
N78E87NW		
N71E82SE		
N76E89SE		
N72E89SE		
N76E88NW		

STATION WB-24
n = 26

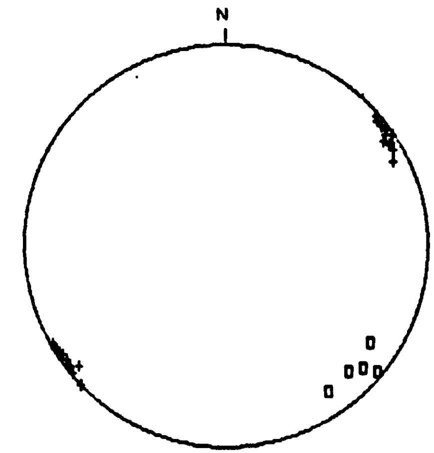

- WB24FA n = 21
- WB24FC n = 5

Schmidt net, lower hemisphere projection

WB24FA	WB24FC	WB24SO
N44W90NE	N46E76NW	SUBHORIZ
N30W85SW	N55E77NW	
N34W89SW	N34E75NW	
N30W89NE	N42E80NW	
N27W82SW	N40E87NW	
N32W85SW		
N36W87NE		
N38W87SW		
N41W88SW		
N31W89NE		
N34W87NE		
N40W87SW		
N34W83SW		
N40W89NE		
N38W88NE		
N33W88NE		
N36W88SW		
N32W86SW		
N32W89NE		
N40W84NE		
N35W86SW		

STATION WB-25

n = 34

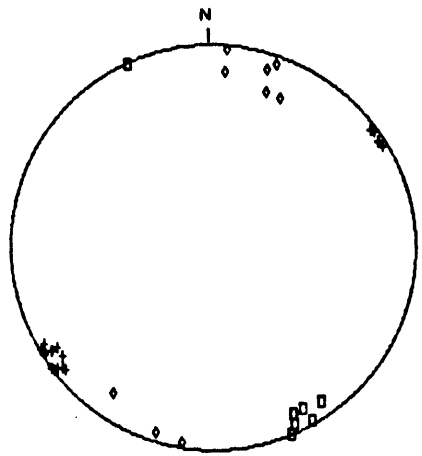

♦ WB25FA n = 18
▪ WB25FD n = 7
◊ WB25FF n = 9

Schmidt net, lower hemisphere projection

WB25FA	WB25FD	WB25FF	WB25SO
N30W89NE	N61E88NW	N70W85SW	SUBHORIZ
N36W87SW	N65E80NW	N85W76SW	
N29W86NE	N66E89SE	N70W70SW	
N38W85NE	N62E80NW	N72W85NE	
N37W89NE	N68E90NW	N65W70SW	
N39W84NE	N66E85NW	N72W81SW	
N32W84NE	N56E82NW	N55W76NE	
N31W88NE		N85W88SW	
N36W90NE		N80W87NE	
N37W87NE			
N32W85NE			
N30W87SW			
N32W81NE			
N31W89NE			
N32W87SW			
N35W81NE			
N32W89NE			
N35W88SW			

STATION WB-26

n = 21

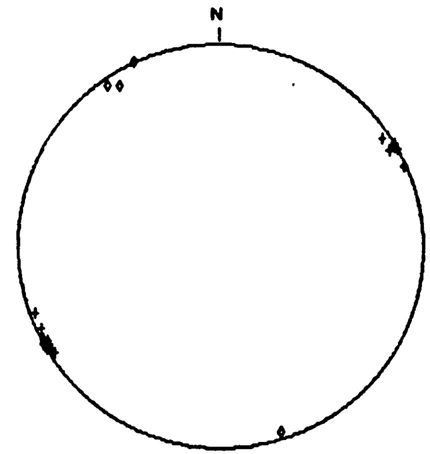

♦ WB26FA n = 17
◊ WB26FD n = 4

Schmidt net, lower hemisphere projection

WB26FA	WB26FD	WB26SO
N20W87NE	N72E86NW	SUBHORIZ
N30W88NE	N58E83SE	
N25W87NE	N65E90SE	
N28W89NE	N55E86SE	
N24W89SW		
N29W87NE		
N31W90NE		
N29W90NE		
N29W90SW		
N31W90SW		
N30W90NE		
N33W87NE		
N30W89SW		
N32W88NE		
N30W86SW		
N34W86SW		
N29W89NE		

STATION WB-27

n = 45

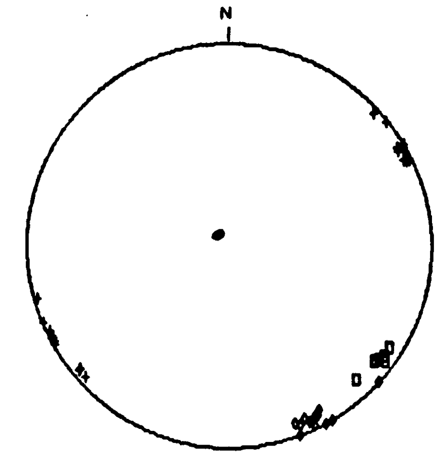

♦ WB27FA n = 22
▪ WB27FC n = 7
◊ WB27FD n = 14
● WB27SO n = 2

Schmidt net, lower hemisphere projection

WB27FA	WB27FC	WB27FD	WB27SO
N23W89NE	N35E83NW	N69E83NW	N58E06SE
N30W89NE	N32E83NW	N66E82NW	N40E06SE
N28W89SW	N38E81NW	N61E90NW	
N31W90SW	N37E82NW	N59E90NW	
N30W89SW	N36E85NW	N65E85NW	
N26W88NE	N37E82NW	N64E88NW	
N43W86NE	N46E80NW	N61E82NW	
N27W86SW		N62E84NW	
N28W88NE		N42E90NW	
N29W88NE		N62E83NW	
N29W88SW		N69E90NW	
N16W88NE		N68E85NW	
N30W86SW		N63E84NW	
N30W89SW		N64E85NW	
N40W85NE			
N40W86NE			
N26W89SW			
N27W89SW			
N39W89SW			
N26W87SW			
N43W87SW			
N31W86SW			

STATION WB-28

n = 15

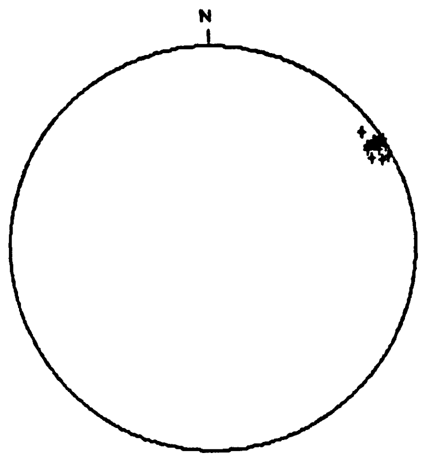

♦ WB28FA n = 15

Schmidt net, lower hemisphere projection

WB28FA	WB28SO
N32W85SW	SUBHORIZ
N32W87SW	
N32W84SW	
N30W89SW	
N32W80SW	
N37W83SW	
N30W85SW	
N27W88SW	
N27W84SW	
N33W85SW	
N29W80SW	
N33W86SW	
N32W88SW	
N33W81SW	
N32W90SW	

STATION WB-29

n = 25

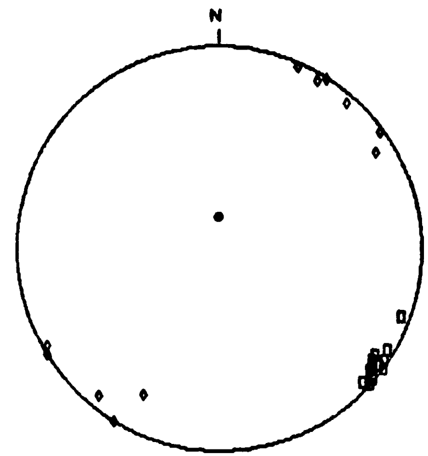

▪ WB29FC n = 13
◊ WB29FF n = 11
● WB29SO n = 1

Schmidt net, lower hemisphere projection

WB29FC	WB29FF	WB29SO
N42E90NW	N51W83NE	N90E13SE
N40E89NW	N36W88SW	
N43E86NW	N63W70NE	
N39E85NW	N58W89SW	
N34E82NW	N59W90NE	
N31E86NW	N49W85SW	
N20E85NW	N67W88SW	
N39E87NW	N30W88NE	
N36E82NW	N32W90NE	
N36E90NW	N32W80SW	
N34E88NW	N60W86SW	
N36E87NW		
N38E85NW		

STATION WB-30

n = 30

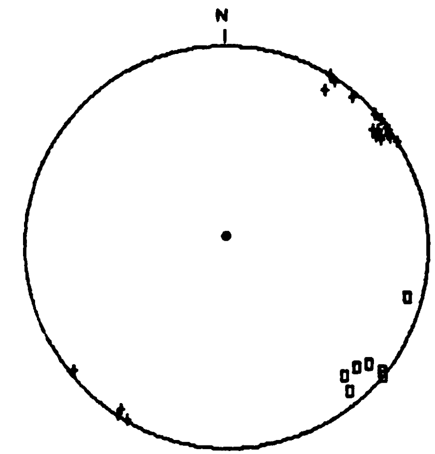

♦ WB30FA n = 22
▪ WB30FC n = 7
● WB30SO n = 1

Schmidt net, lower hemisphere projection

WB30FA	WB30FC	WB30SO
N40W90SW	N43E76NW	N90E05SE
N42W89SW	N40E80NW	
N57W86NE	N48E75NW	
N57W89NE	N50E83NW	
N50W87SW	N40E90NW	
N34W88SW	N39E88NW	
N37W89SW	N15E82NW	
N60W89NE		
N38W85SW		
N39W83SW		
N59W90SW		
N39W88NE		
N35W88SW		
N58W82SW		
N32W90SW		
N37W82SW		
N36W84SW		
N36W90SW		
N38W85SW		
N57W88SW		
N35W83SW		
N37W82SW		

STATION WB-31

n = 31

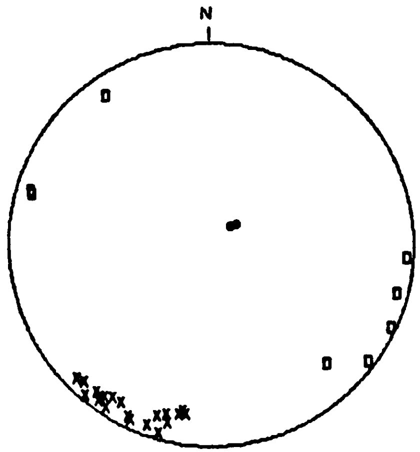

x WB31FB n = 21
▪ WB31FC n = 8
● WB31SO n = 2

Schmidt net, lower hemisphere projection

WB31FB	WB31FC	WB31SO
N76W80NE	N16E81SE	N40W13SW
N52W82NE	N55E79SE	N45W11SW
N80W73NE	N17E82SE	
N74W87NE	N37E86NW	
N55W82NE	N15E84NW	
N54W83NE	N04E86NW	
N54W85NE	N46E71NW	
N60W79NE	N25E87NW	
N81W74NE		
N65W85NE		
N72W78NE		
N54W83NE		
N57W86NE		
N79W75NE		
N47W82NE		
N64W84NE		
N70W84NE		
N45W84NE		
N50W87NE		
N57W79NE		
N75W76NE		

STATION WB-32

n = 30

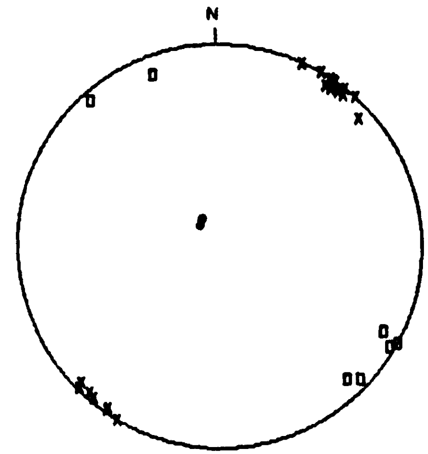

x WB32FB n = 21
▪ WB32FC n = 7
● WB32SO n = 2

Schmidt net, lower hemisphere projection

WB32FB	WB32FC	WB32SO
N59W90SW	N47E80NW	N60E13SE
N53W87SW	N44E85NW	N48E11SE
N56W90SW	N28E80NW	
N47W90SW	N29E90NW	
N55W87NE	N49E85SE	
N65W89SW	N70E80SE	
N54W85SW	N31E87NW	
N55W90SW		
N52W86SW		
N45W89NE		
N59W90NE		
N50W88NE		
N42W83SW		
N51W90SW		
N54W90SW		
N48W87NE		
N55W88NE		
N50W86SW		
N44W86NE		
N52W88SW		
N56W85SW		

STATION WB-33

n = 44

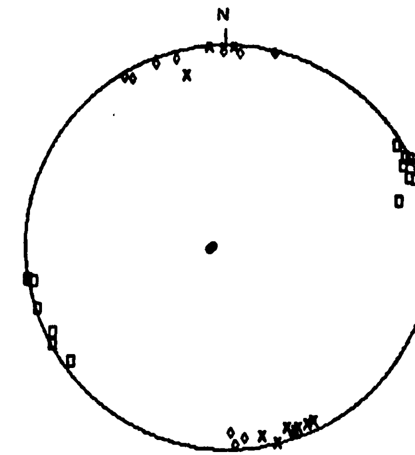

x WB33FD n = 10
▪ WB33FE n = 18
◊ WB33FF n = 14
● WB33SO n = 2

Schmidt net, lower hemisphere projection

WB33FD	WB33FE	WB33FF	WB33SO
N80E84NW	N18W89NE	N59E88SE	N03E06SE
N72E83NW	N25W85SW	N75E86SE	N06W07NE
N76E90NW	N15W76SW	N89E81NW	
N66E85NW	N29W89NE	N76W89SW	
N69E85NW	N09W90NE	N69E87SE	
N88W89SW	N20W88SW	N88W90SW	
N77E76SE	N26W86NE	N89E86SE	
N85E90SE	N09W85SW	N89E90SE	
N70E86NW	N26W90SW	N61E85SE	
N64E85NW	N12W88SW	N71E88NW	
	N10W87NE	N86W86SW	
	N21W85SW	N88E87NW	
	N10W90SW	N85E84NW	
	N36W86NE	N85E84NW	
	N27W88SW		
	N09W90SW		
	N13W90SW		
	N31W87SW		

STATION WB-34

n = 25

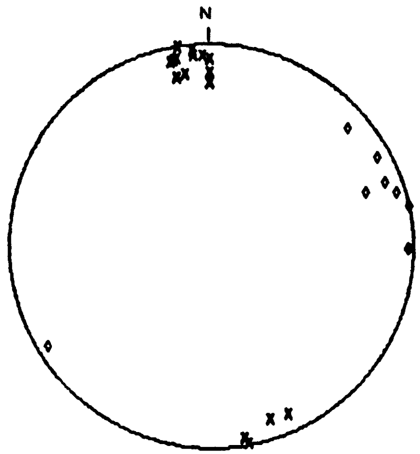

x WB34FD n = 17
◊ WB34FE n = 8

Schmidt net, lower hemisphere projection

WB34FD	WB34FE	WB34SO
N80E83SE	N01E87NW	SUBHORIZ
N79E83SE	N11W90SW	
N90E82SE	N20W81SW	
N85E87SE	N16W85SW	
N90E70SE	N28W83SW	
N78E82SE	N31W84NE	
N85E84SE	N40W79SW	
N81E90SE	N19W70SW	
N82E75SE		
N88E84SE		
N72E79NW		
N66E80NW		
N80E89NW		
N90E75SE		
N79E74SE		
N81E86NW		
N81E86NW		

STATION WB-35

n = 11

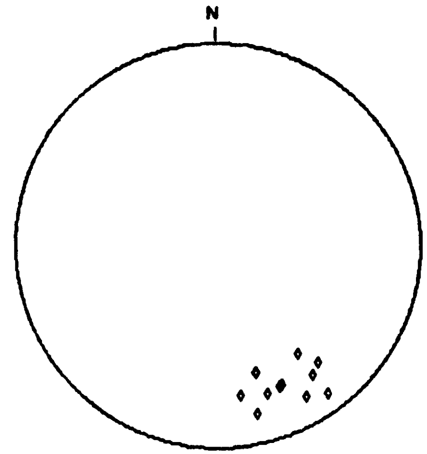

◊ WB35FD n = 11

Schmidt net, lower hemisphere projection

WB35FD	WB35SO
N72E66NW	SUBHORIZ
N60E75NW	
N82E64NW	
N54E68NW	
N66E65NW	
N54E80NW	
N67E65NW	
N74E55NW	
N77E74NW	
N54E56NW	
N50E65NW	

STATION WB-36

n = 20

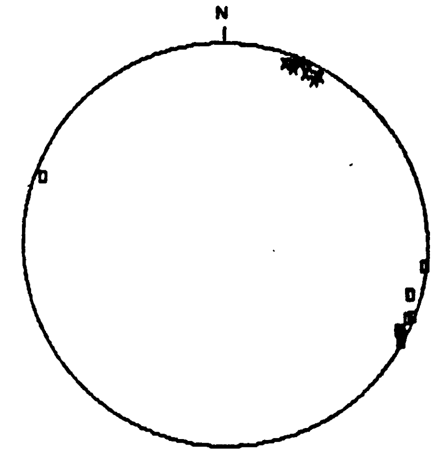

x WB36FB n = 11
▪ WB36FC n = 9

Schmidt net, lower hemisphere projection

WB36FB	WB36FC	WB36SO
N70W85SW	N27E88NW	SUBHORIZ
N65W87SW	N22E87NW	
N68W88SW	N15E84NW	
N65W83SW	N06E89NW	
N61W85SW	N20E86SE	
N62W85SW	N26E85NW	
N69W83SW	N26E86NW	
N62W82SW	N29E89NW	
N65W83SW	N21E89NW	
N68W87SW		
N72W84SW		

STATION WB-37

n = 37

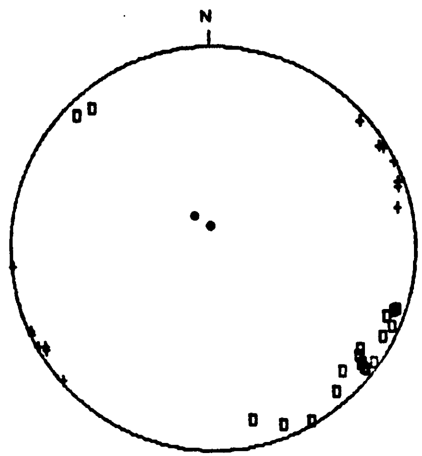

♦	WB37FA	n =	14
▪	WB37FC	n =	21
●	WB37SO	n =	2

Schmidt net, lower hemisphere projection

WB37FA	WB37FC	WB37SO
N18W86SW	N45E83SE	N60E15SE
N25W89SW	N38E82NW	N86E09SE
N12W83SW	N35E77NW	
N41W89NE	N78E76NW	
N29W89NE	N28E84NW	
N31W86SW	N69E83NW	
N40W86SW	N24E86NW	
N19W87SW	N38E82NW	
N30W86NE	N61E88NW	
N30W88SW	N39E86NW	
N25W89NE	N39E82NW	
N05W89NE	N20E84NW	
N24W89NE	N24E86NW	
N31W86NE	N37E78NW	
	N39E84NW	
	N50E80SW	
	N44E77NW	
	N22E81NW	
	N19E85NW	
	N50E83NW	
	N36E87NW	

STATION WB-38

n = 76

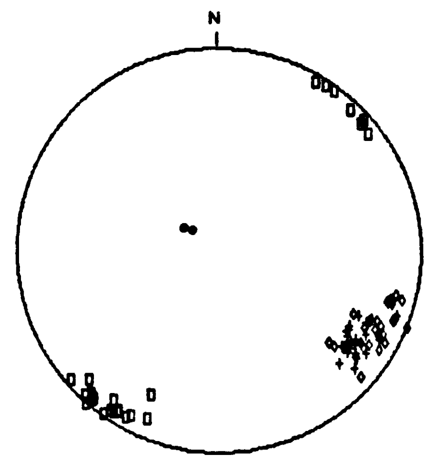

♦	WB38J1	n =	23
▪	WB38J2	n =	25
◊	WB38F1	n =	26
●	WB38SO	n =	2

Schmidt net, lower hemisphere projection

WB38J1	WB38J2	WB38F1	WB38SO
N31E64NW	N65W68NE	N24E74NW	N33E16SE
N32E63NW	N60W86SW	N32E76NW	N39E13SE
N35E77NW	N45W80NE	N38E74NW	
N35E68NW	N54W87SW	N14E79NW	
N20E83NW	N62W82NE	N22E90NW	
N37E69NW	N49W85NE	N25E62NW	
N26E70NW	N67W80NE	N40E60NW	
N30E72NW	N42W86SW	N17E78NW	
N37E67NW	N47W87NE	N33E72NW	
N43E70NW	N57W87SW	N15E83NW	
N41E77NW	N55W80NE	N42E83NW	
N25E65NW	N58W83NE	N29E83NW	
N35E70NW	N57W85NE	N34E75NW	
N29E79NW	N38W83SW	N28E78NW	
N33E69NW	N58W84NE	N25E77NW	
N34E65NW	N50W85NE	N17E76NW	
N33E72NW	N41W87NE	N21E82NW	
N24E71NW	N50W86NE	N28E70NW	
N37E73NW	N55W89NE	N38E67NW	
N38E69NW	N61W84NE	N27E75NW	
N38E66NW	N49W90NE	N27E80NW	
N38E75NW	N48W84NE	N22E82NW	
N30E63NW	N56W85NE	N32E82NW	
	N42W84SW	N16E77NW	
	N47W85SW	N25E71NW	
		N40E63NW	

STATION WB-39

n = 37

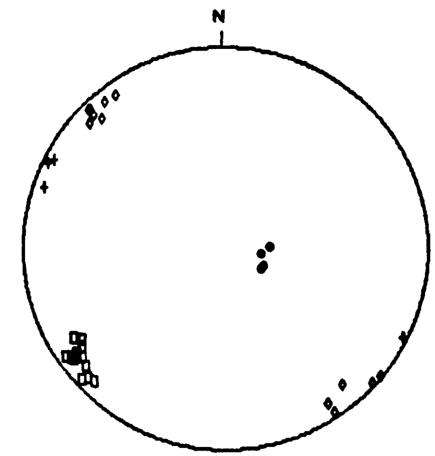

♦	WB39F1	n =	4
▪	WB39F3	n =	17
◊	WB39F5	n =	12
●	WB39SO	n =	4

Schmidt net, lower hemisphere projection

WB39F1	WB39F3	WB39F5	WB39SO
N19E84SE	N45W82NE	N51E83SE	N02W18SW
N26E87SE	N36W81NE	N55E83SE	N29E17NW
N28E85SE	N35W79NE	N43E88NW	N09E15NW
N27E88NW	N35W83NE	N50E78NW	N23E17NW
	N34W85NE	N47E78SE	
	N32W73NE	N46E82SE	
	N40W80NE	N57E87NW	
	N34W75NE	N46E86SE	
	N42W86NE	N46E85SE	
	N37W78NE	N57E81NW	
	N35W82NE	N40E89NW	
	N36W82NE	N43E80SE	
	N30W76NE		
	N36W80NE		
	N43W83NE		
	N36W82NE		
	N35W80NE		

STATION WB-40

n = 14

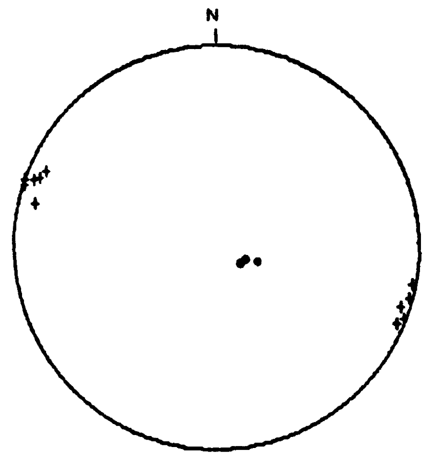

+ WB40F1 n = 11
• WB40SO n = 3

Schmidt net, lower hemisphere projection

WB40F1	WB40SO
N11E88NW	N26E13NW
N13E81SE	N21E17NW
N18E89SE	N36E12NW
N19E90SE	
N24E81SE	
N21E89NW	
N21E82SE	
N20E85SE	
N23E86NW	
N15E88NW	
N18E85NW	

STATION WB-41

n = 32

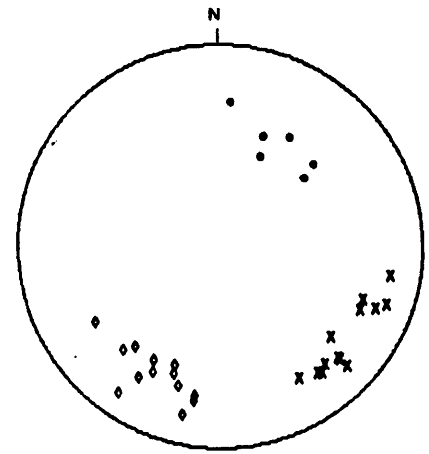

x WB41F5 n = 13
◊ WB41F7 n = 13
• WB41SO n = 6

Schmidt net, lower hemisphere projection

WB41F5	WB41F7	WB41SO
N20E76NW	N73W61NE	N68W49SW
N49E67NW	N55W77NE	N57W54SW
N60E65NW	N69W53NE	N39W45SW
N44E70NW	N80W67NE	N85W61SW
N40E60NW	N58W65NE	N65W41SW
N21E64NW	N77W74NE	N41W52SW
N10E74NW	N80W64NE	
N25E65NW	N60W55NE	
N53E68NW	N47W60NE	
N44E69NW	N31W61NE	
N44E75NW	N50W55NE	
N22E71NW	N70W57NE	
N52E69NW	N62W60NE	

STATION WB-42

n = 15

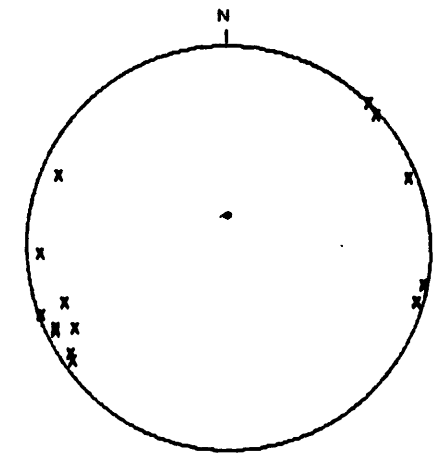

x WB42FE n = 14
• WB42SO n = 1

Schmidt net, lower hemisphere projection

WB42FE	WB42SO
N28W75NE	N90E13SE
N25W84NE	
N20W89NE	
N19W75NE	
N02W83NE	
N34W84NE	
N16E86NW	
N36W85NE	
N11E88NW	
N23E80SE	
N42W88SW	
N26W85NE	
N21W85SW	
N46W90SW	